Classification of a frameshift/extended and a stop mutation in *WT1* as gain-of-function mutations that activate cell cycle genes and promote Wilms tumour cell proliferation

Maike Busch[1], Heinrich Schwindt[1], Artur Brandt[1], Manfred Beier[1], Nicole Görldt[1], Paul Romaniuk[2], Eneda Toska[3], Stefan Roberts[3], Hans-Dieter Royer[1] and Brigitte Royer-Pokora[1,*]

[1]Institute of Human Genetics and Anthropology, Heinrich-Heine University, Medical Faculty, Düsseldorf D-40225, Germany, [2]Institute of Biochemistry and Microbiology, University of Victoria, Victoria, BC, Canada V8P 5C2 and [3]Department of Biological Sciences, University at Buffalo, Buffalo, NY 14260, USA

The *WT1* gene encodes a zinc finger transcription factor important for normal kidney development. *WT1* is a suppressor for Wilms tumour development and an oncogene for diverse malignant tumours. We recently established cell lines from primary Wilms tumours with different *WT1* mutations. To investigate the function of mutant WT1 proteins, we performed *WT1* knockdown experiments in cell lines with a frameshift/extension (p.V432fsX87 = Wilms3) and a stop mutation (p.P362X = Wilms2) of *WT1*, followed by genome-wide gene expression analysis. We also expressed wild-type and mutant WT1 proteins in human mesenchymal stem cells and established gene expression profiles. A detailed analysis of gene expression data enabled us to classify the *WT1* mutations as gain-of-function mutations. The mutant WT1^Wilms2 and WT1^Wilms3 proteins acquired an ability to modulate the expression of a highly significant number of genes from the G2/M phase of the cell cycle, and *WT1* knockdown experiments showed that they are required for Wilms tumour cell proliferation. p53 negatively regulates the activity of a large number of these genes that are also part of a core proliferation cluster in diverse human cancers. Our data strongly suggest that mutant WT1 proteins facilitate expression of these cell cycle genes by antagonizing transcriptional repression mediated by p53. We show that mutant WT1 can physically interact with p53. Together the findings show for the first time that mutant WT1 proteins have a gain-of-function and act as oncogenes for Wilms tumour development by regulating Wilms tumour cell proliferation.

INTRODUCTION

Wilms tumour is a paediatric kidney cancer affecting 1/10 000 children a year. The first protein to be associated with WT development is encoded by the gene *WT1* located on chromosome 11p13 (1,2). *WT1* is mutated in ∼15–20% of all WT and is an important factor for normal kidney development (3). The gene encodes a protein of 52–54 kDa with exons 7 to 10 encoding four C_2-H_2 zinc fingers (ZFs) of the Krüppel type that bind DNA and RNA. The first exons encode a proline–glutamine (Pro/Gln)-rich domain that contains a putative RNA recognition motif and is involved in transcriptional repression and activation, dimerization and nuclear localization (4–7).

Alternative splicing results in four major isoforms, the first leading to inclusion/exclusion of exon 5 and the second to inclusion/exclusion of three amino acids, lysine, threonine and serine (KTS) after exon 9. It was first shown that WT1 lacking KTS binds to a GC-rich EGR1 consensus sequence, as well as to an unrelated TCC repeat motif (8,9). The inclusion of KTS between ZF3 and 4 significantly reduces the DNA-binding

*To whom correspondence should be addressed at: Institute of Human Genetics and Anthropology, Heinrich-Heine-University of Düsseldorf, Postfach 101007, D40001 Düsseldorf, Germany. Tel: +49 2118112350; Fax: +49 2118112538; Email: royer@uni-duesseldorf.de

affinity of WT1 and the +KTS isoform binds to other DNA targets (10). There is also evidence that both WT1 isoforms + and −KTS are involved in post-transcriptional processes (11). The +KTS isoform co-localizes and co-immunoprecipitates with splice factors, and WT1 can modify splicing by interacting with the splice factor U2AF65 (12,13). Using the RNA selection method SELEX and WT1 ZF constructs, three RNA aptamers that are recognized by WT1 were identified (14). Three of four ZFs were necessary, and deletion of ZF1 resulted in reduced and insertion of KTS abolished binding for the RNA targets (14,15). Using these RNA aptamers, Weiss and Romaniuk showed that ZF2 and 3 are necessary for RNA binding (16).

WT1 was found in poly(A)⁺ nuclear RNP from foetal kidneys (17) and in mRNP particles in K562 cells, further pointing to a role in post-transcriptional regulation. There is also strong evidence that WT1 binds to mRNA *in vivo* with an important role of ZF1 in RNA binding (17). *α-Actinin1* (*ACTN1*) was identified as the first cellular RNA target for WT1 (18). In addition, WT1 is also found in the cytoplasm, specifically in cancer cells, suggesting that WT1 could be involved in mRNA export, translation or turnover.

WT1 can form homo- and hetero-dimers with various other proteins and is found in large complexes in Wilms tumours (19,20). WT1 can activate or repress genes depending on the architecture of the promoter; the transcriptional function of WT1 can be modulated through the physical interaction with other proteins (20). The N-terminal transcriptional regulation domain of WT1 was found to bind BASP1, resulting in transcriptional co-suppressor activity (21). WT1 and p53 co-immunoprecipitated in adenovirus E1A-immortalized baby rat kidney cells, and this association resulted in stabilization and increased levels of p53 with enhanced binding to and transactivation of a promoter containing the p53 RGC target sequence. In contrast, repression of a TATA-containing promoter by p53 was inhibited by WT1 (22). The WT1 domain, necessary for binding to p53, was mapped to ZF1 and 2.

Most mutations identified in Wilms tumours lead to a truncated WT1 protein that has lost all or parts of the ZF domain, suggesting that these proteins are impaired in binding to the EGR consensus or the alternative TCC WT1-binding motif. In most cases, however, the N-terminal Pro/Gln-rich repression and activation domain is intact and it is possible that the mutant proteins can still interact with other proteins, thereby modulating their activity. Such a scenario where a truncated mutant WT1 protein inhibits the transcriptional activity of wild-type WT1 has been described (23). In addition, truncated mutant WT1 proteins alter the subcellular localization of the wild-type protein (24). In some cases, the mutations lead to truncation in or after ZF2, 3 or 4, and these proteins may also have retained their RNA-binding capacity or they may bind altered DNA motifs. Recently, a nuclear localization signal in the third ZF was identified that is required for nuclear import (25). We have shown previously that mutant WT1 proteins are predominantly localized to the cytoplasm in Wilms tumours (26) and in Wilms tumour cells as well as in NIH3T3 cells after transfection with mutant *WT1* (27).

We have previously described a method for the successful establishment of Wilms tumour cell lines from Wilms tumours with *WT1* mutations (27). All cell lines carry a homozygous *WT1* mutation owing to loss of heterozygosity of 11p markers.

Only one cell line from a WAGR patient has a hemizygous *WT1* mutation on the remaining allele (Wilms4). These cell lines can be grown for ∼20 passages but do not have an unlimited life span. With this unique Wilms tumour cell culture model system, where both alleles of *WT1* are mutant and no wild-type *WT1* allele is present, we can now begin to study for the first time the function of the mutant WT1 proteins in a homologous system (27). We have previously shown that the Wilms2 cell line has a *WT1* stop mutation in exon 8 leading to a truncation in ZF2 (p.R362X = WT1^Wilms2) and a p.S45Y mutation in *CTNNB1*. The *WT1* frameshift mutation in exon 10 of the Wilms3 tumour cell line leads to an elongation of the WT1 protein by 68 amino acids (p.V432fsX87 = WT1^Wilms3); this cell line is wild type for *CTNNB1*. In Wilms3 cells, the mutant RNA is expressed, the WT1 protein is present in the cytoplasm of the cells, and all isoforms of the WT1^Wilms3 mutant proteins are localized in the cytoplasm of transfected NIH3T3 cells (27). Both WT1 mutant proteins retain the Pro/Gln-rich N-terminus and an intact ZF1. In the WT1^Wilms3 mutant protein, only ZF4 is disrupted, but both + and −KTS isoforms can be synthesized, whereas in Wilms2, ZF2 is truncated and ZF3 and 4 are missing and the stop codon occurs before the KTS alternative splice site. The aim of this study was to functionally characterize these two naturally occurring mutant WT1 proteins and to establish whether they act via gain or loss of function. Here, we report that two cytoplasmically expressed mutant WT1 proteins regulate a number of genes/proteins as revealed by knockdown of mutant *WT1* in the Wilms tumour cell lines. In this work, we show that the mutant proteins retain their ability to interact with p53 and to bind to RNA with a reduced association constant. Loss of *WT1* by knockdown in these cells results in reduced proliferation and reduced expression of genes from the G2/M phase of the cell cycle. Expression of the mutant WT1^Wilms3 protein in mesenchymal stem cells (MSCs) results in up-regulation of the same cell cycle genes, and these genes are not regulated by wild-type WT1, confirming a gain-of-function for the mutant protein.

RESULTS

Intracellular distribution of mutant WT1^Wilms2 protein

Wilms tumour protein WT1 is localized to the nucleus in embryonic and adult tissues (28). We have reported recently that contrary to wild-type WT1, mutant WT1-GFP-fusion proteins from Wilms3 tumour cells are located predominantly in the cytoplasm of transfected NIH3T3 cells (27). The mutation in *WT1*^Wilms3 leads to an extended WT1 protein with additional 68 amino acids at the C-terminus. The positions of mutations in *WT1*^Wilms3 and *WT1*^Wilms2 are shown in Figure 1. WT1^Wilms2 is a truncated protein, and the stop codon occurs before the KTS alternative splice site. Therefore, only the isoforms + and − exon 5 exist. In both Wilms tumour cell lines, the *WT1* mutation is homozygous, i.e. both alleles carry the same mutation and no normal WT1 protein is present in the cells. Here we investigated the intracellular distribution of these proteins in NIH3T3 cells. WT1^Wilms2+exon5- and WT1^Wilms2−exon5-GFP-fusion proteins were expressed in NIH3T3 cells, and a predominant cytoplasmic localization was observed by fluorescence microscopy (Supplementary, Material Fig. S1). In contrast, the wild-type WT1^−/−

and $^{-/+}$ isoforms are exclusively located in the nucleus (Supplementary Material, Fig. S1). Taken together, these results show an important difference between wild-type and mutant WT1 proteins.

Interaction of mutant WT1 proteins with p53

It has been reported that wild-type WT1 protein has the ability to interact with the tumour suppressor p53 (22). Here we wished to examine whether mutant WT1[Wilms2] and WT1[Wilms3] proteins have retained this ability. To investigate whether mutant WT1 proteins interact with p53, HeLa cells that express p53 but no WT1 protein were transfected with plasmids driving expression of GFP, or GFP linked to wild-type WT1, WT1[Wilms2] and WT1[Wilms3]. Preparation of whole cell extracts, followed by immunoprecipitation with antibodies specific for p53 or a control antibody and immunoblotting with a WT1 antibody specific for the N-terminus, demonstrated co-immunoprecipitation of these WT1 proteins with p53. As reported before, wild-type WT1 co-immunoprecipitated with p53 (Fig. 2). Moreover, both WT1[Wilms2] and WT1[Wilms3] retained the ability to interact with p53 (Fig. 2). It is thus possible that mutant WT1 proteins modulate p53 activities in Wilms tumour cells.
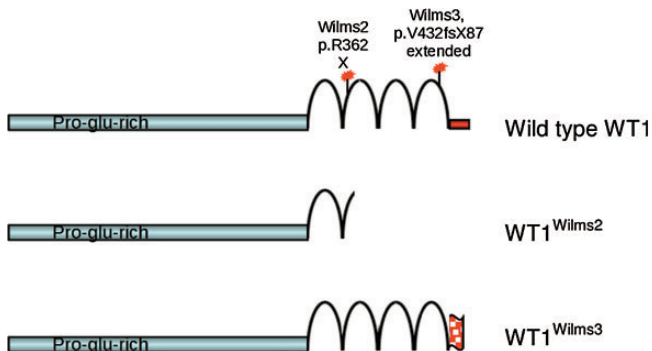

Figure 1. Schematic drawings of wild-type and mutant WT1 proteins. Wild-type WT1 protein (top). Red asterisks indicate the positions of *WT1* mutations that we identified previously in Wilms2 and Wilms3 tumour cells. Truncated WT1[Wilms2] protein (middle). Extended WT1[Wilms3] (bottom). The dotted red flag at the C-terminus of WT1[Wims3] indicates the position of the changed 87 amino acids.

Equilibrium binding of RNA aptamers to the ZF domains of WT1 and Wilms3

As the mutant WT1[Wilms3] protein harbours an intact ZF1, 2 and 3, we wished to study whether the ZF domain from this protein retains its capacity to bind to RNA. The RNA-binding activity of the WT1 ZF domain has been characterized previously using the RNA aptamers RNA22 and RNA38 (29). Here we have determined the affinities of the Wilms3 ZF domains for these two different aptamers using an equilibrium binding assay (Fig. 3). Although the mutation in Wilms3 disrupts proper zinc coordination to finger 4 of the domain, RNA-binding activity is retained but reduced by 4- to 5-fold compared with the wild-type WT1 ZF domain (Fig. 3).

Mutant WT1 proteins are linked to gene regulation in Wilms tumour cells

To gain more insight into the function of mutant WT1[Wilms3] and WT1[Wilms2] proteins, we performed siRNA (si*WT1*) knockdown analyses. First, we tested different *WT1*-specific siRNA oligonucleotides and found that a combination of two siRNAs directed against sequences in exon 6 and the 3′ UTR of *WT1* achieved a very efficient knockdown 48 h after transfection of Wilms3 cells (Fig. 4A). As control a non-silencing siRNA was used. Gene expression profiles were generated using whole-genome microarrays. To identify *WT1* responsive genes, the mean of two biological replicates was determined and the corresponding genes were selected ($P < 0.05$). A 1.5-fold change (fc) relative to the control and a minimal expression of 200 fluorescence intensity was used as cut−off, and we detected 388 genes with increased and 381 genes with decreased expression. The efficiency of *WT1*[Wilms3] knockdown was examined by Q-RT-PCR, and a reduction of *WT1*[Wilms3] expression by 82% was measured (Fig. 4A). Microarray data were validated for selected genes by Q-RT-PCR (Fig. 4B). It is evident that si*WT1* knockdown caused decreased expression of *GDF5* and increased expression of *MESCD2*, *CASP7*, *PODXL1* in Wilms3 tumour cells. We next examined gene expression profiles after si*WT1* knockdown in Wilms2 cells, and the efficiency of *WT1*[Wilms2] knockdown was quantified by Q-RT-PCR (Fig. 4C). We identified 361 genes with increased and 422 genes with decreased expression levels. Microarray data
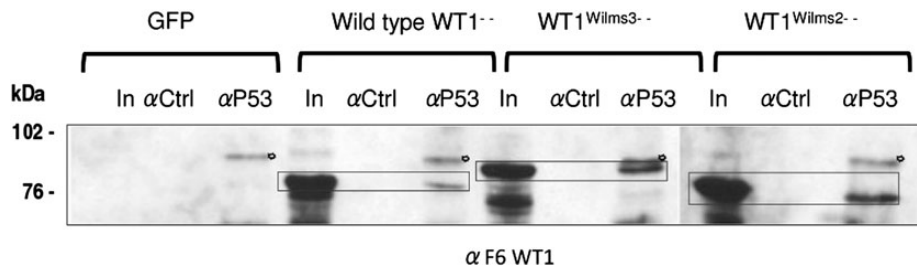

Figure 2. Interaction of p53 and WT1 proteins. Detection of WT1-p53 protein interactions by immunoprecipitation and western blot analysis. HeLa cells were transfected with expression plasmids encoding the WT1-GFP-fusion proteins, wild-type WT1, mutant WT1[Wilms3] and mutant WT1[Wilms2]. As control, cells were transfected with a GFP-expression plasmid alone. Lysates from transfected cells were incubated with control antibodies (lanes, αCtrl) or p53-specific antibodies (lanes, αP53). Immunoprecipitates were resolved by SDS−PAGE and immunoblotted using antibodies specific for the N-terminus of the WT1 protein (αF6WT1). As input controls, 5% of the respective lysates from transfected HeLa cells were loaded on the gel (lanes, In). Asterisk indicates a non-specific band. Wild-type and mutant WT1-GFP-fusion proteins in the input and immunoprecipitated fractions are marked by black boxes.

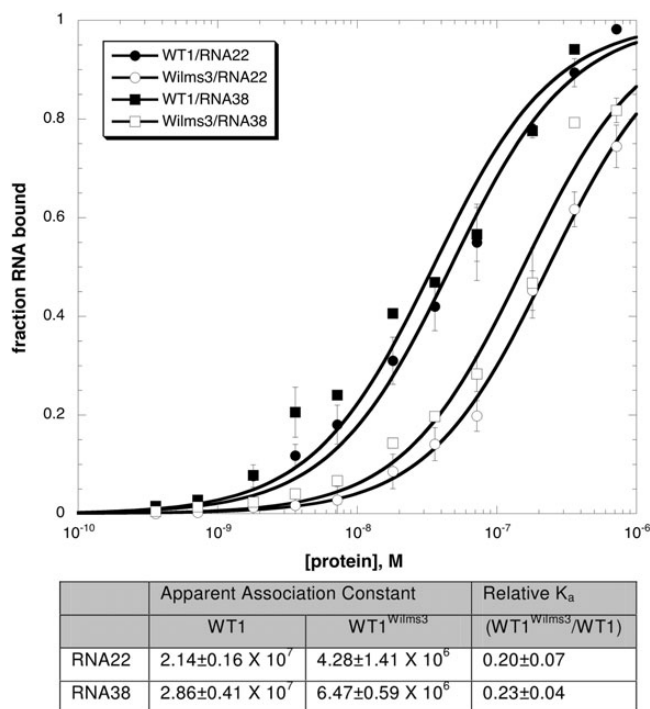|	Apparent Association Constant		Relative K_a
	WT1	WT1^{Wilms3}	(WT1^{Wilms3}/WT1)
RNA22	$2.14\pm0.16 \times 10^7$	$4.28\pm1.41 \times 10^6$	0.20 ± 0.07
RNA38	$2.86\pm0.41 \times 10^7$	$6.47\pm0.59 \times 10^6$	0.23 ± 0.04

Figure 3. Equilibrium binding curves for the binding of the ZF domains of WT1 and Wilms3 to RNA. The affinities of RNA22 and RNA38 were measured using a nitrocellulose filter binding assay. Each line represents the best fit for the formation of a simple bimolecular complex (R values of 0.98–0.99). Each data point is the mean of two independent determinations, with the standard deviation indicated with error bars. The table shows the apparent association constant for wild-type WT1 and mutant WT1^{Wilms3}.

showed a 2.7-fold up-regulation of *PODXL1*, which was validated by Q-RT-PCR (Fig. 4C). Next we compared the si*WT1* gene expression data from Wilms2 and Wilms3 tumour cells and identified a common set of 280 down- and 243 up-regulated genes (Supplementary Material, Fig. S2). These results demonstrate that the mutant WT1 proteins are engaged in regulating gene expression in Wilms tumour cells. Moreover, the data show that truncated WT1^{Wilms2} and extended WT1^{Wilms3} proteins (Fig. 1) regulate similar gene expression programmes.

As this result is of great importance for the field of WT1 research, we wished to confirm our findings by another method. We thus performed lentiviral-mediated sh*WT1* knockdown experiments using Wilms3 tumour cells. The sh*WT1* targets exon 7 of the *WT1* gene, and the most efficient knockdown of *WT1*^{Wilms3} expression (73%) occurred 48 h after infection (Fig. 4D). Gene expression analyses were performed under these conditions, and a scrambled non-silencing shRNA was used as control. A 1.5 fc relative to the control and a minimal expression of 200 fluorescence intensity was used as cut-off. The microarrays identified 1012 genes with increased and 1076 genes with decreased expression levels. Increased expression of *PODXL* and *JARID2* was validated by Q-RT-PCR (Fig. 4E). Taken together our *WT1* knockdown experiments show for the first time that mutant WT1 proteins do have a biological function and this is linked to gene regulation in Wilms tumour cells. The top 100 genes with decreased and increased expression are listed in Supplementary Material, Tables S1

and S2, showing the fold changes of expression relative to the scrambled control.

Mutant WT1 proteins promote expression of genes from the G2/M phase of the cell cycle

To gain more insight into the biological function of the mutant WT1^{Wilms3} protein, we analysed the gene expression data from si*WT1* knockdown experiments using MetaCore, an integrated software suite for functional analysis of biological experimental data. To identify biological processes associated with gene expression data, we used an enrichment analysis of MetaCore pathway maps that represent a set of signalling and metabolic maps covering cellular processes in a comprehensive way. These maps also show functions and interactions of individual genes in a given pathway. We first examined the subset of down-regulated genes obtained from si*WT1* experiments in Wilms3 cells using MetaCore for enrichment of specific pathways and identified highly significant enrichment of several maps from the cell cycle. A list of the ten most significant pathway maps and their *P*-values is summarized in Figure 5A (blue bars). The genes from the cell cycle pathways are listed in Supplementary Material, Table S3, left column. It is evident that these pathways are related to the G2/M phase of cell cycle. The most significant pathway maps 'Cell cycle_Role of APC in cell cycle regulation', 'Cell cycle_Spindle assembly and chromosome separation' and 'Cell cycle_The metaphase checkpoint' operate at the end of G2/ entry into mitosis.

Next, we analysed the subset of genes that were down-regulated after infection of Wilms3 cells with sh*WT1* lentiviruses. The Venn diagram in Supplementary Material, Fig. S3 Panel A, shows that 70 genes are regulated in common in sh*WT1* and si*WT1* knockdown experiments. Enrichment analysis of MetaCore pathway maps revealed 'Cell cycle_The metaphase checkpoint', 'Cell cycle_Chromosome condensation in prometaphase' and 'Cell cycle_initiation of mitosis as highly significant'. A list of the ten top-ranking pathway maps is shown in Figure 5A, orange bars. The most significant pathway map 'Cell cycle_The metaphase checkpoint' is visualized in Figure 5B, and the down-regulated genes are indicated by blue thermometers. The genes corresponding to the cell cycle pathways are listed in Supplementary Material Table S3, right column. Although only 70 identical genes are regulated by si and shRNA, Supplementary Material, Table S3 shows that additional but different genes from the same pathways are regulated in either approach. These data show for the first time that mutant WT1 from Wilms3 tumour cells promote the expression of a significant number of genes from the G2/M phase of the cell cycle. Pathway maps, however, show only selected genes and do not represent all genes of a given biological process. To get a comprehensive overview, we performed a GO process analysis using MetaCore and the subset of down-regulated genes. We identified the most significant biological processes associated with the set of down-regulated genes (Supplementary Material, Fig. S4). These included 'cell cycle' (*P*-value $1.113E-15$), 'mitosis' (*P*-value $1.511E-14$) and 'cell division' (*P*-value $5.459E-14$).

We next performed a MetaCore pathway enrichment analysis of the subset of genes whose expression was down-regulated after siRNA-mediated knockdown of mutant WT1^{Wilms2}. The enrichment analysis of MetaCore pathway maps revealed that 'Cell cycle_Role of APC in cell cycle regulation', 'DNA
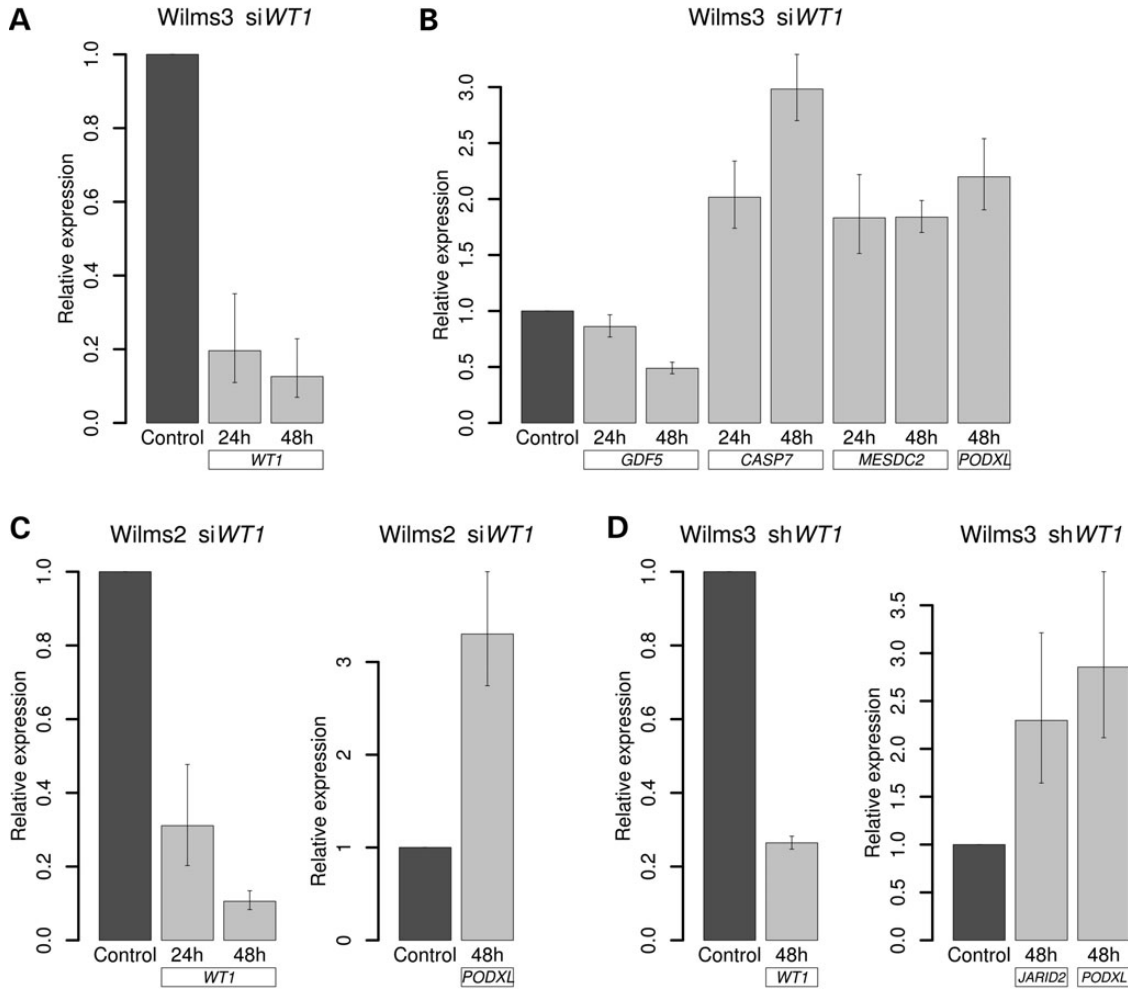
Figure 4. Validation of microarray data from si*WT1* and sh*WT1* knockdown experiments by Q-RT-PCR. All Q-RT-PCR data are displayed relative to a non-silencing si- or shRNA control that is set at 1. Data represent the mean of triplicates, and the standard deviations are indicated for each experiment. PCR reactions were done after transfection of siRNA, and the time points are indicated for each Q-RT-PCR. (**A**) $WT1^{Wilms3}$ expression after treatment with si*WT1*-RNA. (**B**) Validation of *GDF5*, *CASP7*, *MESDC2* and *PODXL* expression after siRNA-mediated *WT1* knockdown in Wilms3 cells. (**C**) $WT1^{Wilms2}$ and *PODXL* expression after treatment with si*WT1*-RNA. (**D**) $WT1^{Wilms3}$ expression 48 h after infection with sh*WT1* lentiviruses (left panel). Expression data are displayed relative to a non-silencing shRNA-lentivirus control that is set at 1. Validation of *JARID2* and *PODXL1* expression in Wilms3 cells infected with sh*WT1* lentiviruses (right panel). Q-RT-PCR was performed 48 h after infection with sh*WT1* lentiviruses.

damage_ATM/ATR regulation of G1/S checkpoint' and 'Cell cycle_the metaphase checkpoint', are the three most significant pathway maps. A list of the ten top-ranking pathway maps and their *P*-values for enrichment is shown in Figure 5C, and the corresponding genes are shown in Supplementary Material, Table S4. We can conclude here that the functions of truncated WT1^{Wilms2} and extended WT1^{Wilms3} proteins are very similar in the context of gene regulation.

WT1^{Wilms3} inhibits the expression of genes from multiple signalling pathways

Next, we wished to examine the biological function of genes that are repressed by mutant WT1^{Wilms3}. We therefore used the subsets of genes that were up-regulated in si*WT1* and sh*WT1* knockdown experiments and performed enrichment analyses of pathway maps using MetaCore. We noticed that the *P*-values for pathway enrichment were lower in si*WT1* than in sh*WT1*

experiments and selected the sh*WT1* data from Wilms3 cells for our analysis. Enrichment analysis by pathway maps identified 'Transcription_Androgen Receptor nuclear signalling' and Cytoskeleton remodelling_TGF, WNT and cytoskeleton remodelling' as most significant. A list of the top-ranking pathway maps is presented in Supplementary Material, Fig. S5 and Table S5. This analysis shows an overrepresentation of enriched pathway maps related to signalling, and we decided to investigate this issue in a more comprehensive fashion. We therefore inspected all pathway maps from the MetaCore database related to signalling and identified a large number of genes that are repressed by mutant WT1. These include *TGFBRII*, *IGF1R*, *AXL*, *MET*, *WNT5* and *FZD6* and the downstream signalling components *DSH*, *CTNNB1*, *AKT*, *DUSP3*, *DUSP16*, *ERK2*, *FAK1*, *MAPK*, *MLCK*, *MYLK1*, *STAT2/3*, *FOS*, *SOS* and others. The proteins encoded by *DUSP3* and *DUSP16* are involved in the negative regulation of Erk signalling and MAPK pathways, respectively (Supplementary Material, Fig. S6). Moreover, WT1^{Wilms3} seems
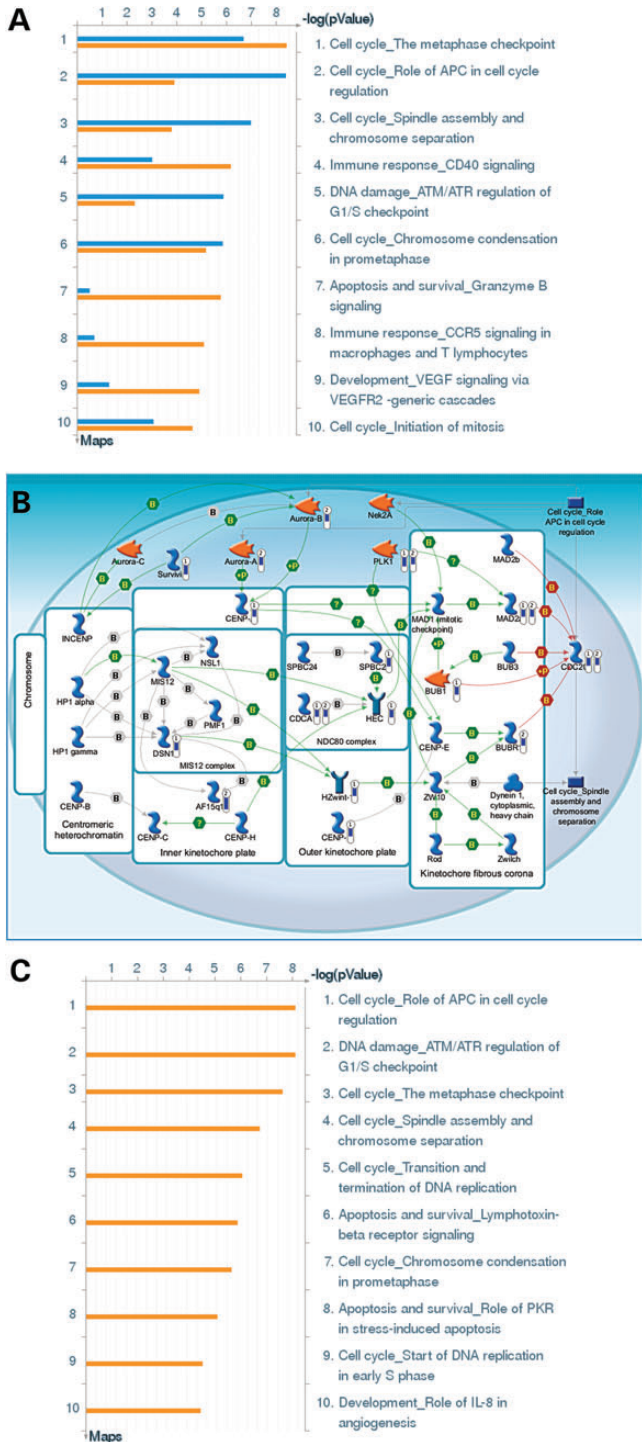
Figure 5. Mutant WT1 proteins control expression of cell cycle genes from the G2/M phase in Wilms2 and Wilms3 tumour cells. (**A**) Enrichment of MetaCore pathway maps in gene expression profiles from Wilms tumour cells after *WT1* knockdown. For enrichment analysis, the subsets of down-regulated genes were used. The height of the blue and orange bars indicates the *P*-values of enrichment for individual pathway maps. Orange bars: *WT1* knockdown in Wilms3 cells after infection with sh*WT1* lentiviruses. Blue bars: *WT1* knockdown in Wilms3 cells after transfection of siRNA. (**B**) MetaCore pathway map 'Cell cycle_The metaphase checkpoint'. Blue thermometers indicate down-regulated genes. The numbers on top of each thermometer refers to individual *WT1* knockdown experiments. 1, sh*WT1* Wilms3 cells; 2, si*WT1* Wilms3 cells. The properties of genes from this pathway are indicated by coloured symbols. These

to repress expression of *CDKN1B* (p27) and *CDKN2B* (p15) genes, negative regulators of progression from the G1 to S phase transition of the cell cycle. A comparison of the si*WT1* with sh*WT1* knock-down experiments is shown in Supplementary Material, Fig. S3, Panel B. The top-ranking pathway 'signal transduction Erk interactions: inhibition of Erk' is identified by the separate analysis of the 70 identical genes that are regulated in both approaches.

Most Wilms tumours with *WT1* mutations also have mutations in *CTNNB1* and in consequence an activated Wnt signalling pathway. However, Wilms3 cells do not carry a *CTNNB1* mutation, and the Wnt/β-catenin pathway is not active as measured by TOP/FOP reporter plasmids (27). To check whether WT1[Wilms3] is involved in regulating expression of genes from Wnt signalling pathways, we used the subset of genes with increased expression in si*WT1* and sh*WT1* experiments and examined the Wnt signalling pathway maps of the MetaCore database. Our analysis revealed that WT1[Wilms3] negatively regulates the expression of several genes from the Wnt signalling pathways including *WNT5*, *DKK1*, *FZD6*, *FZD8*, *MESDC2*, *DSH* (*DVL3*), *CTNNB1*, as well as the downstream target *VIM* (Supplementary Material, Fig. S7). It is known that the regulation of this pathway is highly complex, with several negative regulators being up-regulated in a cell with active Wnt signalling. The up-regulation of ligands, receptors and downstream signalling components upon WT1 removal suggests that the mutant WT1 protein may be a negative regulator of the Wnt signalling pathway. A detailed analysis of this issue will be published elsewhere.

Mutant WT1 proteins promote proliferation of Wilms tumour cells

Our data show that mutant WT1 proteins are involved in regulating the activities of several genes from the G2/M phase of the cell cycle. We therefore investigated whether mutant WT1 proteins also affect the proliferation of Wilms tumour cells. To this end, we determined the proliferation rates of Wilms2 and Wilms3 cells after *WT1* knockdown using sh*WT1* lentiviruses. Figure 6 shows that the sh*WT1* knockdown significantly reduces the proliferation of both Wilms2 ($P = 0.037$) and Wilms3 cells ($P = 0.014$) in comparison with control cells transduced with a non-silencing shRNA. A highly significant inhibition of cell proliferation is also visible in tissue culture dishes 72 and 96 h after infection of Wilms3 cells with sh*WT1* lentiviruses in comparison with the non-silencing control (Supplementary Material, Fig. S8, A). Next, we wished to verify these results by a WST proliferation assay (Supplementary Material, Fig. S8, B). In this assay, cell survival is analysed and we found significantly reduced cells numbers in sh*WT1* expressing cells. This suggests that some cells do not survive without the presence of WT1[Wilms3]. We conclude from these results that the proliferation of Wilms2 and Wilms3 tumour cells is dependent on the activity of mutant WT1[Wilms2] and WT1[Wilms3] proteins. We report here that

symbols are explained by a MetaCore quick reference guide (Supplementary Material, Table S15). Green arrows indicate positive interactions (activation) and red arrows, negative interactions (inhibition). (**C**) Enrichment of MetaCore pathway maps in gene expression profiles from Wilms2 cells after si*WT1* knockdown. For enrichment analysis, the subsets of down-regulated genes were used. The height of the orange bars indicates the *P*-values for enrichment of individual pathway maps.
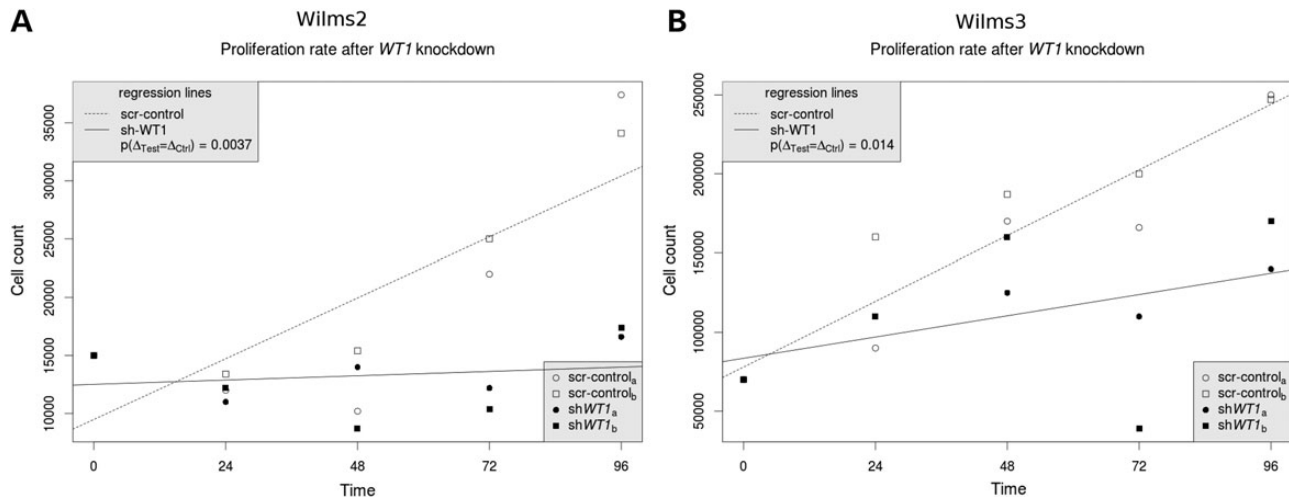
Figure 6. Mutant WT1 proteins promote proliferation of Wilms tumour cells. Wilms2 and Wilms3 cell number after sh*WT1* and scrambled RNA (shC) knockdown at different time points, performed in two independent analyses (a and b), showing a significantly lower median cell count after sh*WT1* knockdown compared with scrambled RNA, Wilms2: $P = 0.037$ (Wilcoxon test) and Wilms3 $P = 0.014$ (Wilcoxon test).

mutant WT1 proteins facilitate the expression of G2/M phase genes, and we asked whether the distribution of cell cycle phases would be altered in Wilms3 tumour cells after sh*WT1* knockdown. To this end, we used the Cycletest[TM] Plus kit in initial experiments and analysed Wilms3 cells 48 h after infection with sh*WT1* lentiviruses using a fluorescence-activated cell sorter (Supplementary Material, Fig. S9). At this time point, we did observe a slight increase of Wilms3 cells in G2/M phase in comparison with the controls; however, apoptosis was not observed in these studies. Future experiments will determine the kinetics of si*WT1* and sh*WT1*-mediated knockdowns in Wilms3 cells and correlate these data with an analysis of cell cycle phases in Wilms3 tumour cells.

WT1[Wilms3] protein modulates the activities of selected transcription factors including p53

Our data show that mutant WT1 proteins are linked to gene regulation. As both Wilms2 and Wilms3 mutant proteins lack a functional DNA binding domain, it was of interest to gain more insight into the underlying molecular mechanisms. To investigate this issue, we used the MetaCore program 'What are the key transcription factors and target genes in my data?' This program uses a database containing all published information regarding transcription factors and their target genes, and the results show which transcription factors play a significant role in individual microarray experiments. First we uploaded the down-regulated genes from sh*WT1* Wilms3 knockdown experiments as the input list. Using these data, the transcription regulation workflow generates sub-networks centred on transcription factors. Sub-networks are ranked by a *P*-value and interpreted in terms of Gene Ontology. The resulted sub-networks of the whole network are displayed in Supplementary Material, Table S6, a network list table, in the order reflecting their statistical significance in terms of *P*-values. The network list shows the top 21 most significant sub-networks centred around CREB1, c-MYC, SP1, YY1, OCT 3–4, GCR-alpha, ESR1, p53, E2F1, Androgen Receptor, HIF1A and others. The

column '*P*-value for enriched transcription factor' indicates the level of significance. The column 'enriched GO processes' lists specific GO processes that were identified in each transcription factor sub-network. For example, the sub-networks centred around CREB1, SP1, YY1, ESR1, p53, E2F1, Androgen Receptor, REL-A p65, ZNF143, NANOG, c-JUN, EGR1, ETS1 and NFKB p50 showed an enrichment of GO processes related to cell cycle and cell proliferation. We also uploaded the up-regulated genes from sh*WT1* Wilms3 knockdown experiments as input list for the MetaCore program 'What are the key transcription factors and target genes in my data?' and identified enriched transcription factors and related GO processes (Supplementary Material, Table S7). It is recognized that different GO processes were identified related to cell metabolism, organismal development, differentiation and many others.

The bioinformatics data provide good evidence that mutant WT1 proteins modulate transcription factor activity, and we wished to further explore this issue and selected p53 as a model system. Wild-type WT1 interacts with p53, and we have shown that mutant WT1[Wilms2] and WT1[Wilms3] proteins also bind to p53 (Fig. 2). Wilms2 and Wilms3 cells express very low levels of p53 protein, which are below the detection limit of western blot analysis. However, we could detect serine 15 (S15), serine 46 (S46) and serine 392 (S392) phosphorylation of p53 using an antibody array (Supplementary Material, Fig. S10, Panel A). To investigate whether p53 is transcriptionally active, we used p53-responsive and p53 non-responsive reporter plasmids (pG13-*Luc* and MG15-*Luc*) that contain p53 wild-type and p53 mutant binding sites. The relative *luciferase* activity of the p53-responsive reporter compared with the p53 non-responsive reporter was highly significant, demonstrating that p53 in Wilms2 and Wilms3 tumour cells is transcriptionally active (Supplementary Material, Fig. S10, Panel B).

The MetaCore program 'What are the key transcription factors and target genes in my data?' revealed that the group of genes ($n = 1076$) that are down-regulated by sh*WT1* contains a subset of 54 p53-target genes where p53 is directly engaged in transcriptional regulation. This information is displayed in a
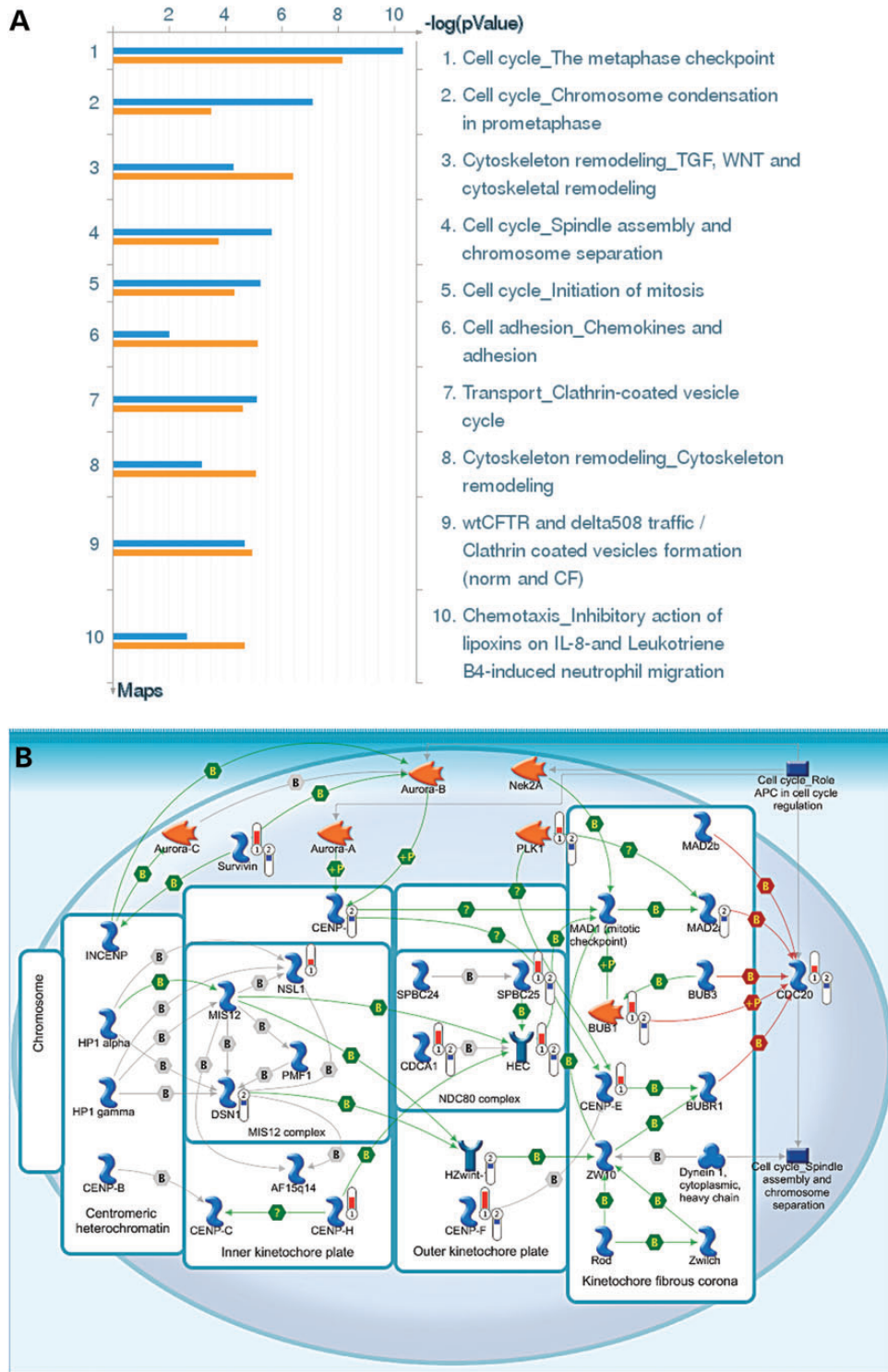
Figure 7. Identification of p53 networks in cohorts of *WT1*^{*Wilms3*} target genes. The MetaCore program 'What are the key transcription factors and target genes in my data' was used to identify p53 networks in subsets of genes whose expressions are either down-regulated (**A**) or up-regulated (**B**) by sh*WT1* knockdown in Wilms3 cells. Blue circles mark down-regulated genes (**A**), and red circles mark up-regulated genes (**B**). The properties of individual genes are indicated by coloured symbols. These symbols are explained in Supplementary Material, Table S15. Green arrows point to genes that are activated by p53 and red arrows to genes that are repressed by p53.

p53 network diagram (Fig. 7A). The p53 network diagram consists of a central p53 node; red arrows are connected to p53-target genes whose expression is inhibited ($n = 20$), and green arrows are connected to genes whose expression is activated by p53 ($n = 34$). If all genes of this p53 network are positively regulated by WT1^{Wilms3}, we can conclude that the mutant WT1 protein can either enhance or antagonize the transcriptional activity of p53. Similar data were obtained when we investigated the group of genes ($n = 1012$) that are up-regulated by sh*WT1*. Here we identified a subset of 44 p53-target genes where 34 are activated and 10 are repressed by p53 (Fig. 7B). These results show that the WT1^{Wilms3} protein has the ability to modulate the transcriptional activity of p53 where it most likely acts either as a co-repressor or co-activator in the context of individual genes. It is important to note that the transcriptional activity of p53 in general is controlled by a highly complex set of co-activators and co-repressors (30).

To further investigate the influence of WT1^{Wilms3} on p53 transcriptional activity, we used a p53-responsive reporter construct (pG13-*Luc*) in transient transfection assays of Wilms3 cells after infection with sh*WT1* lentiviruses (Supplementary Material, Fig. S11). As control, a p53 non-responsive reporter construct (MG 15-*Luc*) was used in transient transfection assays. This initial experiment revealed diminished transcriptional activity of p53 in sh*WT1*-treated Wilms3 cells (Supplementary Material, Fig. S11, right panel). We can conclude that WT1^{Wilms3} acts as a co-activator for p53 in the context of this p53-responsive promoter in pG13-*Luc*.

Classification of WT1 mutations as gain-of-function mutations

Next, we wished to validate the si*WT1* and sh*WT1* knockdown data from Wilms tumour cells by expressing WT1^{Wims3} protein in a cell line devoid of WT1. It is a necessary prerequisite to identify the

spectrum of genes whose expression is controlled by mutant WT1 in order to investigate in a second step whether the mutant protein gained any novel functions in comparison with the wild-type protein. To address these issues, we selected human MSCs as a model system as these do not express WT1. It is important for these experiments to use a cell line related to Wilms tumour cells in order to avoid major context-specific effects. We previously showed that the transcriptomes and differentiation potentials of MSC and our Wilms tumour cells are similar (27). To express wild-type and mutant WT1 in MSCs, we generated lentivirus constructs that express the wild-type $WT1^{+/-}$, $WT1^{++}$, and the mutant $WT1^{Wilms3+/-}$ and $WT1^{Wilms3+/+}$ isoforms. After infection of MSCs, all four lentivirus constructs showed similar expression levels as determined by Q-RT-PCR (Supplementary Material, Fig. S12). Gene expression profiles were established using the same parameters as in *WT1* knockdown experiments. In MSCs infected with $WT1^{Wilms3++}$ lentiviruses, 425 genes were up-regulated and 556 down-regulated. Infection with $WT1^{Wilms3+-}$ lentiviruses caused an up-regulation of 605 and a down-regulation of 755 genes. The top 100 up- and down-regulated genes in MSCs infected with $WT1^{Wilms3+-}$ lentiviruses are listed in Supplementary Material, Tables S8 and S9, respectively. We selected the subset of up-regulated genes from $WT1^{Wilms3+-}$ lentivirus infected MSCs and performed an enrichment analysis of pathway maps using MetaCore. The pathway maps 'Cell cycle_The metaphase checkpoint', 'Cell cycle_Chromosome condensation in prometaphase' and 'Cell cycle_Spindle assembly and chromosome separation' are most significant (Fig. 8A, orange bars). Similar results were obtained using $WT1^{Wilms3++}$ lentiviruses (Fig. 8A, blue bars). These results show that the mutant WT1 protein can activate the expression of a significant number of genes from the G2/M phase of the cell cycle. A comparison of pathway enrichment data after WT1 knockdown in Wilms3 cells (Fig. 5A) with those after

Figure 8. Mutant WT1^{Wilms3} controls expression of cell cycle genes from the G2/M phase in mesenchymal stem cells. (**A**) Enrichment of MetaCore pathway maps in the subset of genes whose expression is induced by *WT1$^{Wilms3++}$* and *WT1$^{Wilms3+-}$* isoforms in MSC. The two isoforms of *WT1^{Wilms3}* were expressed in MSCs using lentiviral constructs. The length of orange bars indicates the *P*-value for enrichment of individual pathway maps in *WT1$^{Wilms3++}$* infected MSCs and blue bars show those for the *WT1$^{Wilms+-}$* isoform. (**B**) Most significant pathway map 'Cell cycle_The metaphase checkpoint': comparison of gene expression levels after sh*WT1* knockdown in Wilms3 cells and lentiviral expression of the mutant *WT1$^{Wilms3+-}$* isoform in MSCs. Red thermometers indicate up-regulated genes by expression of *WT1$^{Wilms3+-}$* in MSC (number 1 on top of the thermometer) and blue thermometers indicate down-regulated genes in sh*WT1* knockdown in Wilms3 cells (number 2 on the top of the thermometer). Properties of individual genes are indicated by coloured symbols. Symbols are explained in a (Supplementary Material, Table S15).
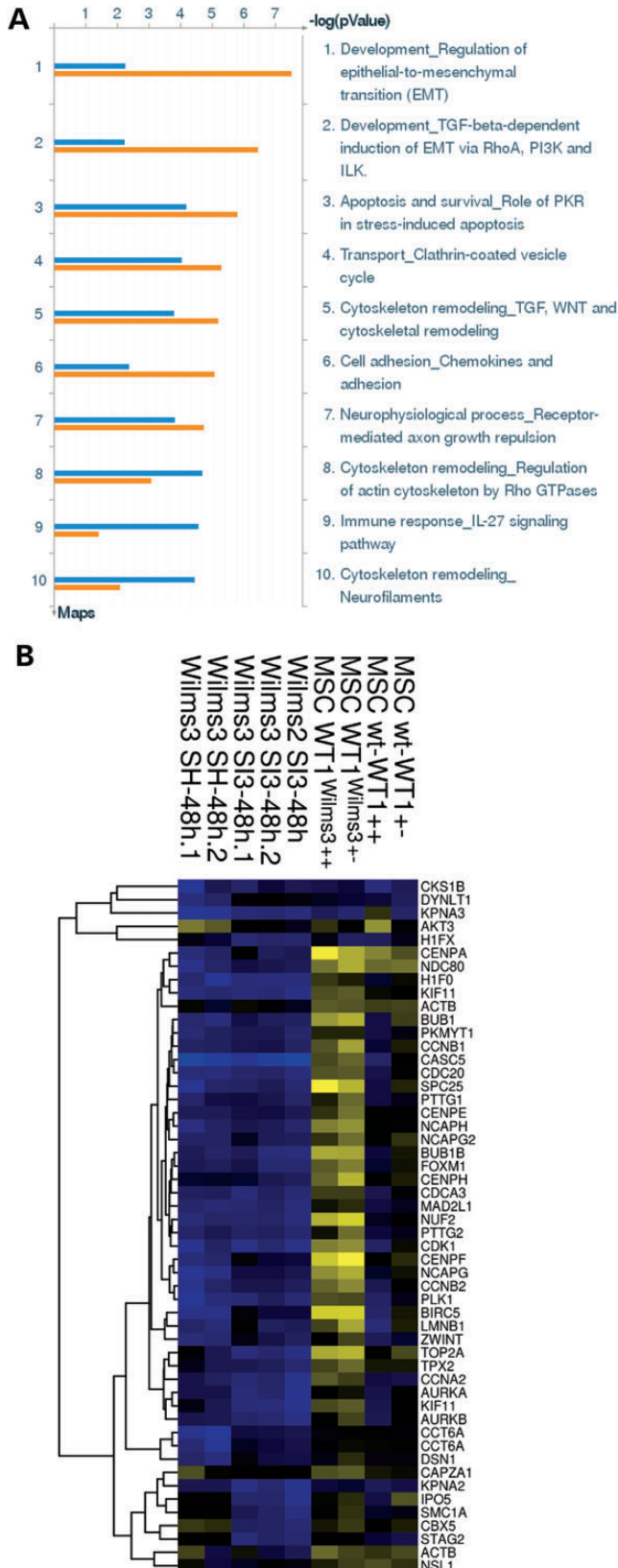
Figure 9. Classification of *WT1^Wilms2* and *WT1^Wilms3* mutations as gain-of-function mutations. (**A**) Enrichment of MetaCore pathway maps for genes induced by wild-type *WT1* in MSCs. The lengths of orange and blue bars correspond to the significance level of individual maps. Orange bars refer to *WT1^{++}*-

WT1^Wilms3 overexpression in MSCs (Fig. 8A) shows complete concordance. This is also demonstrated by the pathway map 'Cell cycle_The metaphase checkpoint' where the sh*WT1* knockdown data from Wilms3 cells and the *WT1*^{Wilms3+−} expression in MSCs have been compared (Fig. 8B). To illuminate quantitative aspects, we compared the fold change values of sh*WT1* down-regulated genes (in Wilms3 cells) with those of *WT1*^{Wilms3+−}-induced genes in MSCs, and a list of common regulated genes is shown in Supplementary Material, Table S10. This gene list comprises a large group of cell cycle genes from G2/M, and it is evident that overexpression of *WT1*^{Wilms3+−} in MSCs induced these genes to a much higher level compared with the fold change repression by sh*WT* knockdown. We conclude here that the mutant WT1 protein is connected to the cell cycle where it is involved in regulating expression of genes that promote the G2/M transition and the proliferation of Wilms tumour cells.

To address the issue whether mutant WT1 proteins gained any function in comparison with wild-type WT1, we infected MSCs with lentiviruses expressing the wild-type *WT1*^{++} and *WT1*^{+−} isoforms. Gene expression analysis was done as described earlier, and we generated datasets of up- and down-regulated genes. Lentiviruses expressing the *WT1*^{++} isoform induced the expression of 882 individual genes, and 690 genes showed reduced expression levels in MSC. Infection with *WT1*^{+−} lentiviruses was associated with an up-regulation of 425 and a down-regulation of 696 genes. The top 100 up- and down-regulated genes in MSCs infected with *WT1*^{Wilms3+−} lentiviruses are listed in Supplementary Material, Tables S11 and S12, respectively. We then performed a MetaCore pathway enrichment analysis using the datasets for the *WT1*^{++} and *WT1*^{+−} isoforms (Fig. 9A). This figure shows that identical pathway maps are significantly enriched in gene expression profiles after infection of MSCs with the two WT1 isoforms. The *P*-values for pathway enrichment are indicated for *WT1*^{++} and *WT1*^{+−} by orange and blue bars, respectively (Fig. 9A). Although identical pathways were enriched, the *P*-values indicate subtle differences between the *WT1*^{++} and *WT1*^{+−}-dependent gene expression profiles. For the *WT1*^{++} isoform 'Development regulation of epithelial to mesenchymal transition' and for the *WT1*^{+/−} isoform 'Cytoskeleton remodeling_Regulation of actin cytoskeleton by RHO GTPases' were the most significant pathway maps. Next, we looked for any enrichment of cell cycle pathway maps in gene expression

induced gene expression data and blue bars to gene expression data induced by the *WT1*^{+−} isoform. There was no significant enrichment of any pathway map related to the cell cycle. (**B**) Gene expression data from MSCs infected with *WT1*^{Wilms3+−} lentiviruses show proof of gain-of-function. To generate the heatmap, we selected a subset of genes from the cell cycle whose expression was down-regulated by si*WT1* and sh*WT1* knockdown in Wilms tumour cells and compared their expression levels in diverse experiments that are indicated in the Figure. The colour corresponds to the log ratio of *WT1* knockdown versus scrambled control transfected cells (blue negative log ratio and yellow positive log ratio). Lanes Wilms3 SH-48h.1 and Wilms3 SH-48h.2 are biological replicates of lentivirus-mediated sh*WT1* knockdown in Wilms3 cells, 48h after infection, and are log ratios versus scrambled RNA transduced cells. Wilms3 SI3-48h.1 and Wilms3 SI3-48h.2 are biological replicates of si*WT1*-mediated knockdown in Wilms3 cells 48 h after transfection versus non-silencing RNA. Wilms2 SI3-48h corresponds to si*WT1*-mediated knockdown in Wilms2 cells. MSC *WT1*^{Wilms3++} and MSC *WT1*^{Wilms3+−} refer to MSCs infected with lentiviruses expressing two isoforms of mutant *WT1*^{Wilms3}, and MSC wt-*WT1*^{++} and MSC wt-*WT1*^{+−} refer to MSCs infected with lentiviruses expressing two isoforms of wild-type *WT1*, expressed as log ratios versus control virus-transduced cells.

data from $WT1^{++}$ and $WT1^{+-}$-infected MSCs and visually inspected the top 50 enriched pathway maps (Supplementary Material, Fig. S13). We did not find any pathway map related to the cell cycle in this analysis. We can conclude from this data that mutant WT1 differs from wild-type WT1 by the capacity to regulate 'cell cycle genes'. This function is novel, and therefore, these mutations can be classified as gain-of-function mutations.

To confirm this result at the level of individual genes, we generated a heat map using the down-regulated 'cell cycle genes' from *WT1* knockdown experiments (Fig. 9B). The lanes labelled Wilms3 and Wilms2 show all experimental data of *WT1* knockdown experiments using either si*WT1* or sh*WT1* lentiviruses and are represented as log ratios versus scrambled control RNAs. The lanes MSC $WT1^{Wilms3}$ show the log ratios of gene expression data after infection of MSC with lentiviruses expressing mutant $WT1^{Wilms3}$, versus control virus-transduced cells, and the lanes MSC wt-*WT1* show the gene expression levels after infection of MSC with lentiviruses expressing wild-type WT1 versus control virus. The heat map visualizes our results and shows that all 'cell cycle genes' that are repressed by si*WT1* and sh*WT1* knockdown approaches are up-regulated by lentivirus-mediated expression of mutant $WT1^{Wilms3}$ in MSC. Moreover,

lentivirus-mediated expression of wild-type *WT1* in MSC failed to activate expression of these genes. We conclude that the *WT1* mutations that have been identified in Wilms2 and Wilms3 tumour cells are gain-of-function mutations. This gain-of-function phenotype of mutant $WT1^{Wilms3}$ is also evident when the top 100 genes induced by $WT1^{Wilms3+-}$ and wt$WT1^{+-}$ lentiviruses are compared (Supplementary Material, Table S13). In this cohort of genes, only *APOL6* and *MNS1* are induced by both lentiviruses (intensity >200). It is very interesting to note that in the cohort of the top 100 genes that were down-regulated by $WT1^{Wilms3+-}$ and wt$WT1^{+-}$ lentiviruses (Supplementary Material, Table S14), most genes are repressed by both lentivirus types. This is also visualized in the Venn diagrams shown in Fig 10. Here the large overlap of genes down-regulated by mutant and wild-type WT1 is evident (Fig. 10A), whereas only a smaller set of genes is up-regulated by both lentiviruses (Fig. 10B). We can conclude that the gain-of-function mutation in mutant Wilms tumour proteins is confined to transcriptional activation, whereas transcriptional repression is mediated by both, the wild-type and mutant WT1 proteins. Future work is needed to exactly work out how transcriptional activation and repression by mutant WT1 is brought about.
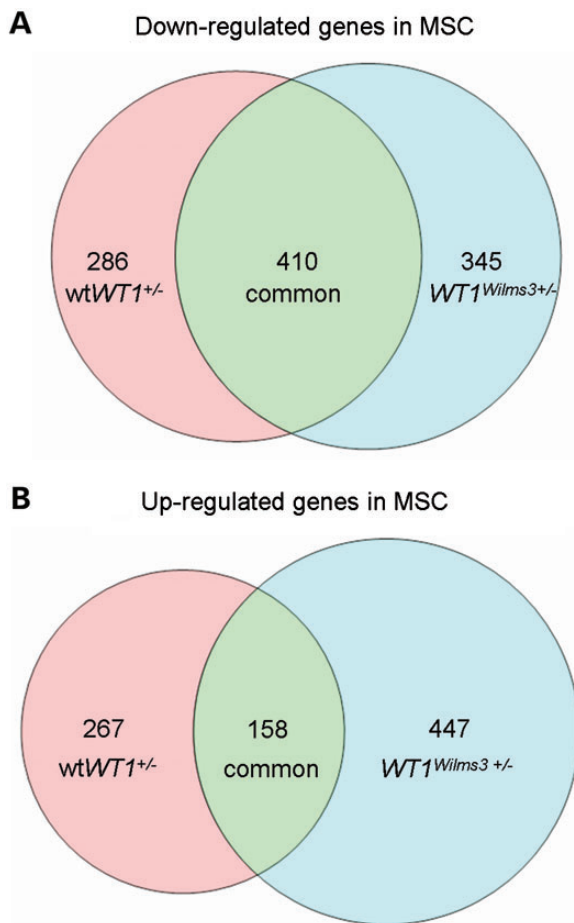
DISCUSSION

Most *WT1* mutant Wilms tumours have lost the wild-type *WT1* allele, following Knudson's two-hit hypothesis for the inactivation of a tumour suppressor gene (31,32). In contrast in many adult human tumours, *WT1* is highly expressed and sometimes mutations are found, suggesting that it acts as an oncogene (32,33). Some Wilms tumours with *WT1* mutations express the mutant RNA and protein (27). Wilms tumour-derived Wilms2 and Wilms3 cell lines were used here to address the question whether *WT1* mutations have an impact for the biology of Wilms tumours. To investigate whether mutant WT1^{Wilms2} and WT1^{Wilms3} proteins gained a new function (gain-of-function mutation), we compared the gene expression profiles of MSCs, infected with lentiviruses expressing mutant and wild-type *WT1*, and found that mutant WT1 proteins activate the expression of a large number of genes from the G2/M phase of the cell cycle, whereas wild-type *WT1* was unable to do so. These data show unequivocally that $WT1^{Wilms2}$ and $WT1^{Wilms3}$ mutations are gain-of-function mutations. This result is particularly interesting because it contradicts the currently accepted model that mutant WT1 proteins contribute to Wilms tumour development because they no longer function as tumour suppressor (32). Mutant $WT1^{Wilms2}$ and $WT1^{Wilms3}$ promote the proliferation of Wilms tumour cells in tissue culture, and it has been shown for a variety of human cancers that their growth and survival can be impaired by the inactivation of a single oncogene, a phenomenon termed oncogene addiction (34).

This gain-of-function mutation in $WT1^{Wilms3}$ is illustrated in a Venn diagram (Fig. 10A and B). Here we compared the datasets of up-regulated genes from MSCs infected with $WT1^{Wilms3+-}$ and wt*WT1*. Gain-of-function is demonstrated by the blue area in Figure 10B. However, the picture is more complex as there are genes that are regulated by both, wt*WT1* and the mutant protein (green area). In addition, as expected there are quite a number of genes that are induced by wt*WT1* only (pink area).

Figure 10. Comparison of mutant and wild-type *WT1*-dependent gene expression in MSCs. Lentiviruses expressing the $+-$ isoforms of mutant $WT1^{Wilms3}$ and wild-type *WT1* were used in these experiments. The expression data are displayed in Venn diagrams. (**A**) Comparison of down-regulated genes and (**B**) up-regulated genes.

We also compared the top 100 induced genes from MSCs infected with wt$WT1^{+-}$ and $WT1^{Wilms3+-}$ lentiviruses. Here it is evident that amongst these, only two genes were induced in common (Supplementary Material, Table S13). This clearly demonstrates that gain-of-function is the dominant consequence of this mutation. Different results are evident in the group of down-regulated genes (Fig. 10A). The green area indicates that a large fraction of genes is repressed by wt$WT1^{+-}$ and $WT1^{Wilms3+-}$ in MSCs. We also compared the top 100 repressed genes from MSCs infected with wt$WT1^{+-}$ and $WT1^{Wilms3+-}$ lentiviruses and found that the majority of genes was repressed by both, the wt$WT1$ and the mutant protein (Supplementary Material, Table S14). Taken together these data show that a novel transcription activation function is the major phenotype of the $WT1$ mutation in Wilms3 cells. The repression function of wtWT1 and the mutant protein may be explained by the presence of the Pro/Gln-rich transregulatory and dimerization domain in the N-terminal domain. This domain also contains a putative RNA recognition motif (5,8,17), and mutant Wilms3 protein has retained its ability to bind to RNA aptamers, albeit with reduced affinity. Therefore, the mutant proteins can interact and modulate the function of other proteins and/or bind to RNA as well. However, the mechanisms by which the mutant proteins exert these functions remain to be identified.

It is interesting to note that a leukaemia-associated mutant WT1 protein devoid of the ZF domain, WT1(delZ), has also gained new functions (35). Whereas WT1 inhibited the proliferation of haematopoietic progenitor cells (36), the WT1(delZ) protein promoted expansion of human haematopoietic progenitor cells in tissue culture. $WT1$ mutations were detected in $10-15\%$ of adult AML cases at diagnosis, and the presence of $WT1$ mutations is an independent predictor of poor clinical outcome (35). Gene expression profiling revealed that WT1(delZ) expression was associated with increased gene expression levels of certain genes related to proliferation and decreased expression levels of genes related to myeloid differentiation.

Mutant WT1 controls genes from the G2/M phase of the cell cycle. For example, the expression of *BIRC5*, *BUB1*, *CCNB1*, *CCNB2*, *CDC20*, *CDK1*, *CENPF*, *PLK1* and *UBE2C* was down-regulated by sh$WT1$ in Wilms3 cells and up-regulated in MSCs infected with lentiviruses expressing the $WT1^{Wilms3+-}$ isoform. It is remarkable that *CCNB1*, *CCNB2* and *CDK1* are amongst these genes as they are key regulators of cell cycle progression in G2/M phase. The most significant transcriptional signature of cancer cells and malignant tumours is the up-regulation of cell cycle and proliferation-related genes (37). An analysis of gene expression data from a large variety of human cancer types identified a core proliferation cluster (core PC) predominantly consisting of genes from the G2/M phase of the cell cycle (38). A comparison of our gene expression data with those from the core PC showed a high degree of overlap. The core PC consists of 46 genes and 21 of these genes showed reduced expression in lentiviral sh$WT1$ knockdown experiments. Similar results were obtained by si$WT1$ knockdown in Wilms2 and Wilms3 cells. We can conclude from these data that the $WT1$ gain-of-function mutations in Wilms2 and Wilms3 cells are oncogenic events affecting gene expression of important cell cycle regulators and in consequence increased proliferation of Wilms tumour cells. This is supported by our $WT1$ knockdown experiments, which showed that the mutant WT1 proteins promote proliferation of

Wilms2 and Wilms3 tumour cells. This finding provides convincing experimental evidence that the $WT1$ mutations may contribute to the development of Wilms tumours *in vivo*.

A large number of cell cycle regulatory genes are also principal targets of p53-mediated repression (38,39). Transcriptional repression mediated by p53 is complex and involves other transcription factors like E2F1 and NFY (38). Mutant WT1 proteins can activate the transcription of cell cycle genes that are repressed by p53. These include *CCNB1*, *CDK1*, *PLK1*, *CDC20*, *MAD2a* and others (39–43). The promoter of the *Cyclin B* (*CCNB1*) gene for example contains a p53 head-to-tail response element, and binding of a p53 dimer to this response element is sufficient to abrogate transcription (40). We show here that mutant WT1 can activate *CCNB1* and *CCNB2* expression, and this suggests that the mutant protein can antagonize the repression function of p53 at the *Cyclin B* promoter. Future experiments will elucidate how the activation of the *Cyclin B1* gene expression is brought about. WT1 interacts with p53 and modulates its function (22). Mutant WT1^{Wilms2} and WT1^{Wilms3} proteins can bind to p53 *in vitro*, and it is possible that this property enables WT1^{Wilms3} to neutralize p53-dependent repression of the *Cyclin B* promoter *in vivo*. The major phenotype of the WT1 mutation is the gain of a transactivation function, and an interaction of mutant WT1 with p53 at the *Cyclin B1* promoter might enable this transactivation function to overcome repression by p53. Another possible scenario is the sequestration of p53 by mutant WT1 in the cytoplasm, resulting in loss of p53 function in the nucleus. In the context of this issue, it is important to study in future experiments, whether mutant WT1 proteins can be detected in the nucleus, even in minor amounts. Our immunofluorescence analysis (Supplementary Material, Fig. S1) and recent work (27) showed a predominant cytoplasmic localization of mutant WT1 proteins. Despite of this, it is possible that small amounts of these proteins are transported to the nucleus by a piggyback mechanism after association with other nuclear proteins. This is a speculative argument at this stage; however, a mutant WT1 protein lacking the ZF domain (WT1-delZ) was identified in nuclei of transfected osteosarcoma cells (44).

We have shown that Wilms2 and Wilms3 proteins are able to interact with RNA. It is possible that cytoplasmic localization of mutant WT1 proteins affects gene expression by altering the metabolism of RNA in the cells. This is, however, a complex issue and investigations addressing the functions of cytoplasmic mutant WT1 proteins are beyond the scope of the current work. In addition, we provided evidence based on an analysis using the MetaCore program 'What are the key transcription factors and target genes in my data?' that mutant WT1 modulates the activities of selected transcription factors also in the context of cell cycle-related gene expression. Again these results revealed an additional level of complexity, and this will be addressed in future studies.

Our $WT1$ knockdown data show that mutant WT1 inhibits the expression of a large number of genes from signalling pathways including several members of the canonical Wnt and planar cell polarity signalling pathways. The regulation of these pathway activities is complex, and in some cases, gene expression levels of inhibitors (e.g. A*XIN2*) can be up-regulated in the active state of the pathway. To ultimately determine activity of a given pathway of interest, functional studies are required,

which are beyond the scope of this investigation and will be part of future work. With regard to Wnt signalling, it is important to note that wild-type WT1 inhibits Wnt signalling because it competes with TCF4 for binding to CBP (45). Moreover, depletion of wild-type WT1 results in up-regulation of *CTNNB1* expression and WT1 negatively regulates Wnt signalling in Sertoli cells (46). Mutant *WT1^Wilms3^* down-regulates *CTNNB1* expression that might also inhibit the Wnt signalling pathway. In this context, it is of special interest to note that Wilms3 cells express wild-type *CTNNB1*. Therefore, Wilms3 tumour cells can survive without *CTNNB1* mutations that are a common phenotype of Wilms tumours where *WT1* is mutated. Mutant WT1^Wilms3^ was classified as a gain-of-function mutation with oncogenic potential, and the *WT1* knockdown data showed that the growth and survival of Wilms3 tumour cells is dependent on the expression of WT1^Wilms3^.

Furthermore, several genes that are repressed by mutant WT1 are involved in chromatin modification and some are positive and negative regulators of MAPK signalling. It was reported that wild-type WT1 negatively regulates the RAS/MAPK signalling pathway by inducing the expression of MKP3 (DUSP6), a phosphatase and negative regulator of this pathway (47). Here we found that mutant WT1 inhibits the expression of the dual specificity phosphatase genes *DUSP3* and *DUSP16*. Another group of genes that are down-regulated by mutant WT1 are differentiation regulating genes, e.g. *GREM2*, *HMOX1*, *MYO5a*, *MYO9B*, *GDNF*, *NES*, *NKX3−1*, *PODXL*, *HGFL* and *SNPO*. By using mouse models, it was shown that *PODXL* is a WT1 target gene with high expression levels in podocytes and highly differentiated kidney epithelial cells (48). *PODXL* gene expression is induced by WT1 and repressed by p53 (49). Wild-type WT1 activates *PODXL* by direct binding to its promoter, and WT1 and PODXL are co-expressed in the developing kidney (50). We have reported recently that WT1 and BASP1 interact with the promoter of *PODXL*, BASP1 inhibiting WT1. During differentiation, BASP1 promoter binding is down-regulated and in consequence WT1 can activate *PODXL1* gene expression (51). Since the expression of *PODXL* is inhibited by *WT1^Wilms3^* and *PODXL* expression is increased during kidney differentiation, one could argue that mutant WT1 keeps the tumour cells in an undifferentiated or less differentiated state.

In summary, we have identified novel gain-of-function mutations of *WT1* that occurred *in vivo* during the development of Wilms tumours in patients. These mutations may drive tumour development as they promote cell proliferation in Wilms tumour cells. This result is of special interest for the biology of Wilms tumours as an ablation of W*t1* alone does not induce Wilms tumours in transgenic mice. However, in a transgenic mouse model with carrying a *WT1* truncation mutation (396 stop), one animal developed a WT (52). It is interesting that in this Wilms tumour, one allele carried the targeted mutation and the other allele showed an exon 9 skipping event. Therefore, this tumour developed when both *WT1* alleles carried mutations, corresponding to our Wilms tumour cell lines, where both alleles harbour the same the mutation (52). These data are reminiscent of the situation with another tumour suppressor, p53. A mouse model for pancreatic cancer revealed that a mutant form of p53 had an increased tumorigenicity through a gain-of-function mechanism. In this case, mutant p53 had extra functions over and above the loss of p53 in a tumour model (53).

MATERIALS AND METHODS

Cell culture

Human mesenchymal stem cells were purchased from Lonza and maintained in MSCGM (Lonza). The primary Wilms tumour cell lines Wilms2 and Wilms3 were described previously (27) and were cultivated in MSCGM with a medium change every 3 days.

Plasmids and lentiviral expression vectors

Full-length human wild-type and mutant (p.V432fsX87) *WT1* genes with an optimal Kozak sequence in front of the start ATG were cloned through PCR from mutant *WT1^Wilms3++^* and *WT1^Wilm3+−^* isoforms in pCRII-TOPO vectors and from wild-type *WT1^++^* and *WT1^+−^* isoforms in pDNA3.3-Topo-TA vectors. Primers for the PCR were Kozak-*WT1*-for (5′ AACGAATTCAC CACCATGGGCTCCGACGTGCGG 3′) and wt-*WT1*-rev (5′ GT TGAATTCTCAAAGCGCCAGCTGGAGTT 3′) or mut-*WT1*-rev (5′ CAGTCGACTCAACTAAAAGTAGGCAGGGC 3′). The PCR products were cloned into the pCRII-TOPO vector and excised by digestion with EcoRI (wild-type *WT1*) or KpnI/XbaI (mutant *WT1*) and ligated into the pENTR4 vector [Addgene, 17 424 (54)], digested with the same restriction enzymes. The wild-type and mutant *WT1* isoforms were finally cloned into the pLenti CMV Puro Dest vector [Addgene, 17 452 (54)] through the Gateway Technology as described in the 'Gateway LR Clonase II Enzyme Mix' protocol (Invitrogen). As a control for the transduction of expression vectors, a FOP luciferase pLenti X1 dest puro vector was used, containing the FOP expression cassette, cloned from the M51 super 8 FOP Flash [Addgene (55)]. All vector constructs were verified by sequencing.

The construction of a plasmid vector used to express the ZF domain of wild-type WT1 has been described previously (56). The cDNA used in this study to express the ZF domain (−KTS) of Wilms3 was constructed by the polymerase chain reaction (PCR) using an upstream primer at the start of ZF 1, containing a NcoI recognition sequence and a downstream primer including the termination codon for the Wilms3 reading frame, containing a EcoRI recognition sequence. PCR products were digested with NcoI and EcoRI and ligated into plasmid pET30a, digested with the same restriction enzymes. The NcoI site puts the Wilms3 cDNA in frame with the vector-included his-tag. Plasmids were isolated from appropriate colonies, and the correct plasmid constructs were confirmed by DNA sequencing.

The 'Mission shRNA Plasmid DNA' with a pLKO.1-puro backbone used in the *WT1* knockdown experiments and the non-mammalian shRNA control used in all transduction experiments were purchased from Sigma−Aldrich; sh*WT1* (exon7, TRCN0000040067) and sh scrambled (SHC002).

Production of lentiviral viral particles, transduction and siRNA transfection

For virus production, HEK293 T cells were transfected with 6 μg of each plasmid DNA: packaging vector pczVSV-G (57), pCD NL-BH (57) and the desired expression vector in the presence of 45 μg PEI (Polyethyleneimine, branched, Aldrich). As internal transfection control, a lentiviral GFP-expression Vector (pCL7EGwo, obtained from Dr H. Hanenberg) was transfected

in each experiment. The medium was changed after 1 day to IMDM with 10% FCS and 1% penicillin/streptomycin, and 48 h after transfection, viral supernatants were harvested, filtered (0.45 μm), concentrated by centrifugation and cryo-conserved.

WT1 knockdown experiments were performed with (1) transfection with siRNA oligonucleotides (si*WT1*) and (2) infection with lentiviruses expressing shRNA (sh*WT1*). For si*WT1* knockdown, Wilms2 and Wilms3 cells were seeded in 24-well plates (4×10^4 cells/well), transfected after 24 h with the 'HiPerfect transfection reagent' (Qiagen) with a combination of two different siRNAs (Qiagen: Hs_WT1_1_HP in 3′ UTR and Hs_WT1_8_HP in exon 6) and a non-silencing control siRNA, Alexa Fluor 488 labelled (Qiagen). Total RNA was isolated at the indicated time points.

For sh*WT1* experiments, Wilms3 cells were seeded in a 6-well plate (5×10^4 cells/well). After 24 h, the cells were infected with sh*WT1* lentiviruses or as control with lentiviruses expressing a non-silencing shRNA in the presence of polybrene (5 μg/ml, H9268, Sigma), and the medium was changed after 4 h. RNA was isolated 48 h after transduction. All experiments were performed in duplicates.

Overexpression of wild-type and mutant proteins in MSCs was achieved by seeding 1×10^5 MSC in 6-well plates and infection after 24 h with 2 ml of the respective lentiviruses in the presence of polybrene (1 mg/ml). For a biological replicate, the experiments were done in duplicates. The medium was changed after 24 h to MSCGM, and RNA was isolated at 48 h. The negative control was a scrambled lentiviral vector.

RNA isolation, gene expression analysis and Q-RT-PCR

Total RNA was isolated after *WT1* knockdown or overexpression using the RNeasy Mini Kit (Qiagen). Labelling of total RNA in the Two-Colour format was performed as described by the manufacturer (Agilent Technologies). The cRNA was hybridized to 4×44 K 'Whole Human Genome Oligo Microarrays' (Agilent, V1), and 'Spike-In positive controls' (Agilent) were added as internal controls. Expression arrays were scanned (Agilent Technologies Scanner G2505B) and quantified using the Agilent Feature Extraction V10.1.1.1 Software. The software package LIMMA (R-library, bioconductor, http://www.R-project.org) was used for statistical analysis and the search for differentially expressed genes. The gene expression data were submitted and are found at GEO, GSE54635.

For Q-RT-PCR analyses, cDNAs were synthesized using TaqMan Reverse Transcription Reagents (Applied Biosystems). All Q-RT-PCR experiments were performed in triplicates using the TaqMan gene expression assay probes from Applied Biosystems for *WT1* (Hs00240913_m1), *MESDC2* (Hs00398059_m1), *GDF5* (Hs00167060_m1) *CASP7* (Hs01029847-_m1), *PODXL* (hCG18687) and *JARID2* (Hs1004460_m1) with the TaqMan Universal PCR master Mix (no AmpEraseUNG) or Brilliant II QPCR Master Mix with Low Rox (Agilent Technologies). In the si*WT1* experiments, the expression levels were normalized with the *18S*RNA (Hs99999901_s1), in the sh*WT1* experiments with *GAPDH* (4333764 T). The *WT1* knockdown was normalized versus *ACTB* (4333762F) and the overexpression versus *RER1* (Hs00199824_m1). The reason for using these different calibrator probes was that we noted a regulation of the calibrator gene in some of these experiments, and therefore, we have

identified a new gene that was basically never regulated in any of our gene expression studies: *RER1*. The si*WT1* Q-RT-PCRs were run on an ABI PRISM 7900HT, and the Q-RT-PCRs from sh*WT1* and expression of *WT1* in MSC were run on a Mx3000P Sequence Detection System (Stratagene).

Microarray data analysis

Microarray data analysis was performed using the MetaCore software suite (http://thomsonreuters.com/metacore/) to identify biological processes associated with gene expression profiles. For analysis of gene expression profiles, normalized microarray data were manually curated before uploading individual data files. We selected only named genes from datasets and used a cut-off of 200 fluorescence intensity and a fold change of 1.5. The Agilent Identification numbers of selected genes were then uploaded and analysed using the MetaCore software program Enrichment Analysis (EA) for Datasets:

Enrichment analysis consists of mapping gene IDs of the dataset(s) of interest onto gene IDs in entities (terms) of built-in functional ontologies represented in MetaCore™/MetaDrug™ by pathway maps and networks. Mapping procedure involves calculating statistical relevance of the matches found. We use both ontologies, which are the result of our in-house extensive classification effort, and public ontologies such as Gene Ontology (GO, www.geneontology.org). Ontologies are represented by canonical pathway maps, cellular process networks, disease biomarker networks, drug target networks, toxicity networks and metabolic networks. GO ontologies include GO processes, GO molecular functions and GO localizations.

Statistical relevance of the found ontology matches is calculated as *P*-value, or a probability of a match to occur by chance, given the size of the database. The lower the *P*-value, the higher is the 'non-randomness' of finding the intersection between the dataset and the particular ontology. That, in turn, translates into a higher rating for the term matched. In particular, the more genes/proteins belong to a process/pathway, the lower the *P*-value. MetaCore program 'What are the key transcription factors and target genes in my data?' uses a database containing all published information regarding transcription factors and their target genes. We uploaded the up- or down-regulated genes from sh*WT1* knockdown experiments in Wilms3 cells as the input list. The transcription regulation workflow generates sub-networks centred on transcription factors. Sub-networks are ranked by a *P*-value and interpreted in terms of Gene Ontology. The resulted sub-networks of the whole network are displayed in Supplementary Material, Table S6 and Table S7, a network list table, in the order reflecting their statistical significance in terms of *P*-values.

Cell proliferation after *WT1* knockdown

For the determination of the proliferation rates of Wilms2 and Wilms3 cells after *WT1* knockdown, 5×10^4 cells per well were seeded in MSCG medium in a 6-well plate. After transduction with sh*WT1* and scrambled control lentiviral particles, the cells were counted in a Neubauer chamber 24 h, 48 h, 72 and 96 h. Each time point was analysed in duplicate. RNA was extracted from these cells for gene expression analysis.

Expression and purification of recombinant ZF proteins

Preparations of N-terminal his-tagged ZF proteins were carried out as described previously (58). Protein purity was confirmed by SDS-polyacrylamide gel electrophoresis (PAGE), and the concentration of each protein preparation was determined by the method of Bradford.

Radiolabelling of RNA ligands and equilibrium binding of RNAs to ZF proteins

Preparation of radiolabelled RNA aptamers by *in vitro* transcription was as described previously (29). The apparent association constants for the binding of radiolabelled RNAs to ZF proteins were determined using a double-filter binding assay. The binding buffer consisted of 20 mM Tris–HCl pH 7.5 (20°C), 5 mM $MgCl_2$, 100 mM KCl, 10 μM $ZnCl_2$, 0.5 mM Tris (2-carboxyethyl)phosphine hydrochloride, 100 μg/ml BSA and 1 μg/ml polydIdC. The affinity of each ZF protein for RNA was determined using three or more independent assays. Apparent dissociation constants (K_d) for the binding of the mutant and wild-type proteins to RNA were calculated by fitting the data to a simple bimolecular equilibrium model using the general curve fitting function of Kaleidagraph software (Synergy Software, Reading, PA, USA) and the following equation:

$$\frac{[\text{RNA-protein}]}{[\text{RNA}]_{\text{total}}} = \frac{[\text{protein}]_{\text{total}}}{[\text{protein}]_{\text{total}} + K_d} \qquad (1)$$

where $[\text{RNA}]_{\text{total}} << K_d$ and $[\text{RNA-protein}]/[\text{RNA}]_{\text{total}}$ is reported as the fraction of RNA bound. Association constant (K_a) values were derived as the reciprocal of the measured K_d values and are reported as the mean of three independent determinations with the associated standard deviations. Relative affinities were arrived at by dividing the apparent K_a for the mutant protein by the apparent K_a for the wild-type protein determined in parallel, or by dividing the apparent K_a for the mutant RNA by the apparent K_a for the wild-type RNA determined in parallel. The errors for relative affinities are given by the expression $\sigma = \{(\sigma 1/M1)^2 + (\sigma 2/M2)^2\}^{1/2} \times M2/M1$, where M1 and M2 are the respective association constants for wild-type and mutant protein and the σ values are the corresponding standard deviations for these determinations.

Analysis of endogenous p53 activity in Wilms cells

Endogenous p53 activity in Wilms3 cells was measured with the p53-responsive reporter pG13-*Luc* [13 p53 binding sites, Addgene, 16 442 (59)] and the non-responsive reporter pG15-*Luc* [15 mutant p53 binding sites, Addgene, 16 443 (59)]. As control, Wilms3 cells were transfected with a promoter-less pGL3-basic *luciferase* vector. All cells were co-transfected with pGL4.75 (*Renilla-Luc*) for normalization. Cells were lysed after 24 h in 1× Passive Lysis Buffer (Promega), and the *luciferase* activity was measured with the Beetle-/Renilla-Juice Big Kit (PJK GmbH, Germany) as described by the manufacturer. The relative p53 *luciferase* activity was determined as quotient of the *firefly-luciferase* and *renilla-luciferase* activity. The analysis was performed in triplicates.

For the determination of the status of the p53 protein, cell lysates from Wilms2 and Wilms3 cell lines were used for probing the Human Phospho-Kinase Array (Catalog # ARY003B, R&D). The analysis was performed as described by the manufacturer (R&D).

Protein interaction of WT1 and p53

HeLa cells were cultured in Dulbecco's modified Eagle's medium and transfected with Effectene (Qiagen) with pAcGFP vectors expressing N-terminally GFP-tagged WT1^{Wilms3} or WT1^{Wilms2} or wild-type WT1 fusion proteins (27). Preparation of whole cell extracts and IP western blot were carried out as described previously (60). Antibodies anti-WT1 (F6) and anti-p53 (DO1) sc-126 were obtained from Santa Cruz Biotechnology.

SUPPLEMENTARY MATERIAL

Supplementary Material is available at *HMG* online.

Conflict of Interest statement. None declared.

REFERENCES

1. Call, K.M., Glaser, T., Ito, C.Y., Buckler, A.J., Pelletier, J., Haber, D.A., Rose, E.A., Kral, A., Yeger, H. and Lewis, W.H. (1990) Isolation and characterization of a zinc finger polypeptide gene at the human chromosome 11 Wilms' tumor locus. *Cell*, **60**, 509–520.
2. Gessler, M., Poustka, A., Cavenee, W., Neve, R.L., Orkin, S.H. and Bruns, G.A. (1990) Homozygous deletion in Wilms tumours of a zinc-finger gene identified by chromosome jumping. *Nature*, **343**, 774–778.
3. Hastie, N.D. (1993) Wilms' tumour gene and function. *Curr. Opin. Genet. Dev.*, **3**, 408–413.
4. Madden, S.L., Cook, D.M., Morris, J.F., Gashler, A., Sukhatme, V.P. and Rauscher, F.J. III (1991) Transcriptional repression mediated by the WT1 Wilms tumor gene product. *Science*, **253**, 1550–1553.
5. Kennedy, D., Ramsdale, T., Mattick, J. and Little, M. (1996) An RNA recognition motif in Wilms' tumour protein (WT1) revealed by structural modelling. *Nat. Genet.*, **12**, 329–331.
6. Englert, C. (1998) WT1—more than a transcription factor? *TIBS*, **23**, 389–393.
7. Roberts, S.G.E. (2005) Transcriptional regulation by WT1 in development. *Curr. Opin. Genet. Dev.*, **15**, 542–547.
8. Rauscher, F.J., Morris, J.F., Tournay, O.E., Cook, D.M. and Curran, T. (1990) Binding of the Wilms' tumor locus zinc finger protein to the EGR-1 consensus sequence. *Science*, **250**, 1259–1262.
9. Wang, Z.-Y., Qiu, Q.Q., Enger, K.T. and Deuel, T. (1993) A second transcriptionally active DNA-binding site for the Wilms tumor gene product, WT1. *Proc. Natl. Acad. Sci. USA*, **90**, 8896–8900.
10. Bickmore, W.A., Oghene, K., Little, M.H., Seawright, A., van Heyningen, V. and Hastie, N.D. (1992) Modulation of DNA binding specificity by alternative splicing of the Wilms tumor wt1 gene transcript. *Science*, **257**, 235–237.

11. Morrison, A.A., Viney, R.L. and Ladomery, M.R. (2008) The post-transcriptional roles of WT1, a multifunctional zinc-finger protein. *Biochim. Biophys. Acta.*, **1785**, 55–62.

12. Larsson, S.H., Charlieu, J.P., Miyagawa, K., Engelkamp, D., Rassoulzadegan, M., Ross, A., Cuzin, F., van Heyningen, V. and Hastie, N.D. (1995) Subnuclear localization of WT1 in splicing or transcription factor domains is regulated by alternative splicing. *Cell*, **81**, 391–401.

13. Davies, R.C., Calvio, C., Bratt, E., Larsson, S.H., Lamond, A.I. and Hastie, N.D. (1998) WT1 interacts with the splicing factor U2AF65 in an isoform-dependent manner and can be incorporated into spliceosomes. *Genes Dev.*, **12**, 3217–3225.

14. Bardeesy, N. and Pelletier, J. (1998) Overlapping RNA and DNA binding domains of the wt1 tumor suppressor gene product. *Nucleic Acids Res.*, **26**, 1784–1792.

15. Caricasole, A., Duarte, A., Larsson, S.H., Hastie, N.D., Little, M., Holmes, G., Todorov, I. and Ward, A. (1996) RNA binding by the Wilms tumor suppressor zinc finger proteins. *Proc. Natl. Acad. Sci. USA*, **93**, 7562–7566.

16. Weiss, T.C. and Romaniuk, P.J. (2009) Contribution of individual amino acids to the RNA binding activity of the Wilms' tumor suppressor protein WT1. *Biochemistry*, **48**, 148–155.

17. Ladomery, M.R., Slight, J., Mc Ghee, S. and Hastie, N.D. (1999) Presence of WT1, the Wilm's tumor suppressor gene product, in nuclear poly(A)(+) ribonucleoprotein. *J. Biol. Chem.*, **274**, 36520–36526.

18. Morrison, A.A., Venables, J.P., Dellaire, G. and Ladomery, M.R. (2006) The Wilms tumour suppressor protein WT1 (+KTS isoform) binds alpha-actinin 1 mRNA via its zinc-finger domain. *Biochem. Cell Biol.*, **84**, 789–798.

19. Iben, S. and Royer-Pokora, B. (1999) Analysis of native WT1 protein from frozen human kidney and Wilms' tumors. *Oncogene*, **18**, 2533–2536.

20. Roberts, S.G.E. (2006) The modulation of WT1 transcription function by cofactors. *Biochem. Soc. Symp.*, **73**, 191–201.

21. Carpenter, B., Hill, K.J., Charalambous, M., Wagner, K.J., Lahiri, D., James, D.I., Andersen, J.S., Schumacher, V., Royer-Pokora, B., Mann, M., Ward, A. and Roberts, S.G.E. (2004) BASP1 is a transcriptional cosuppressor for the Wilms' tumor suppressor protein WT1. *Mol. Cell. Biol.*, **24**, 537–549.

22. Maheswaran, S., Englert, C., Bennett, P., Heinrich, G. and Haber, D.A. (1995) The WT1 gene product stabilizes p53 and inhibits p53-mediated apoptosis. *Genes Dev.*, **9**, 2143–2156.

23. Reddy, J.C., Morris, J.C., Wang, J., English, M.A., Haber, D.A., Shi, Y. and Licht, J.D. (1995) WT1-mediated transcriptional activation is inhibited by dominant negative mutant proteins. *J. Biol. Chem.*, **270**, 10878–10884.

24. Englert, C., Vidal, M., Maheswaran, S., Ge, Y., Ezzell, R.M., Isselbacher, K.J. and Haber, D.A. (1995) Truncated WT1 mutants alter the subnuclear localization of the wild-type protein. *Proc. Natl. Acad. Sci. USA*, **92**, 11960–11964.

25. Depping, R., Schindler, S.G., Jacobi, C., Kirschner, K.M. and Scholz, H. (2012) Nuclear transport of Wilms' tumour protein Wt1 involves importins α and β. *Cell Physiol. Biochem.*, **29**, 223–232.

26. Schumacher, V., Schuhen, S., Sonner, S., Weirich, A., Leuschner, I., Harms, D., Licht, J., Roberts, S. and Royer-Pokora, B. (2003) Two molecular subgroups of Wilms' tumors with or without WT1 mutations. *Clin. Cancer Res.*, **9**, 2005–2014.

27. Royer-Pokora, B., Busch, M., Beier, M., Duhme, C., de Torres, C., Mora, J., Brandt, A. and Royer, H.-D. (2010) Wilms tumor cells with WT1 mutations have characteristic features of mesenchymal stem cells and express molecular markers of paraxial mesoderm. *Hum. Mol. Genet.*, **19**, 1651–1668.

28. Mundlos, S., Pelletier, J., Darveau, A., Bachmann, M., Winterpacht, A. and Zabel, B. (1993) Nuclear localization of the protein encoded by the Wilms' tumor gene WT1 in embryonic and adult tissues. *Development*, **119**, 1329–1341.

29. Zhai, G., Iskandar, M., Barilla, K. and Romaniuk, P.J. (2001) Characterization of RNA aptamer binding by the Wilms' tumor suppressor protein WT1. *Biochemistry*, **40**, 2032–2040.

30. Coutts, A.S. and La Thangue, A.B. (2005) The p53 response: emerging levels of co-factor complexity. *Biochem. Biophys. Res. Commun.*, **331**, 778–785.

31. Schumacher, V., Schneider, S., Figge, A., Wildhardt, G., Harms, D., Schmidt, D., Weirich, A., Ludwig, R. and Royer-Pokora, B. (1997) Correlation of germ-line mutations and two-hit inactivation of the WT1 gene with Wilms tumors of stromal-predominant histology. *Proc. Natl. Acad. Sci. USA*, **94**, 3972–3977.

32. Huff, V. (2011) Wilms' tumours: about tumour suppressor genes, an oncogene and a chameleon gene. *Nat. Rev. Cancer*, **11**, 111–121.

33. Yang, L., Han, Y., Suarez Saiz, F. and Minden, M.D. (2007) A tumor suppressor and oncogene: the WT1 story. *Leukemia*, **21**, 868–876.

34. Weinstein, I.B. and Joe, A. (2008) Oncogene addiction. *Cancer Res.*, **68**, 3077–3080.

35. Vidovic, K., Ullmark, T., Rosberg, B., Lennartsson, A., Olofsson, T., Nilsson, B. and Gullberg, U. (2013) Leukemia associated mutant Wilms' tumor gene 1 protein promotes expansion of human hematopoietic progenitor cells. *Leuk Res.*, **37**, 1341–1349.

36. Svedberg, H., Richter, J. and Gullberg, U. (2001) Forced expression of the Wilms tumor 1 (WT1) gene inhibits proliferation of human hematopoietic CD34(+) progenitor cells. *Leukemia*, **15**, 1914–1922.

37. Whitfield, M.L., George, L.K., Grant, D. and Perou, C.M. (2006) Common markers of proliferation. *Nat. Rev. Cancer*, **6**, 99–106.

38. Brosh, R. and Rotter, V. (2010) Transcriptional control of the proliferation cluster by the tumor suppressor p53. *Mol. Biosyst.*, **6**, 17–29.

39. Spurgers, K.B., Gold, D.L., Coombes, K.R., Bohnenstiehl, N.L., Mullins, B., Meyn, R.E., Logothetis, C.J. and McDonnell, T.J. (2006) Identification of cell cycle regulatory genes as principal targets of p53-mediated transcriptional repression. *J. Biol. Chem.*, **281**, 25134–25142.

40. Lipski, R., Lippincott, D.J., Durden, B.C., Kaplan, A.R., Keiser, H.E., Park, J.H. and Levesque, A.A. (2012) p53 Dimers associate with a head-to-tail response element to repress cyclin B transcription. *PLoS One*, **7**, e42615, 1–9.

41. McKenzie, L., King, S., Marcar, L., Nicol, S., Dias, S.S., Schumm, K., Robertson, P., Bourdon, J.C., Perkins, N., Fuller-Pace, F. and Meek, D.W. (2010) p53-dependent repression of polo-like kinase-1 (PLK1). *Cell Cycle*, **9**, 4200–4212.

42. Kidokoro, T., Tanikawa, C., Furukawa, Y., Katagiri, T., Nakamura, Y. and Matsuda, K. (2008) CDC20, a potential cancer therapeutic target, is negatively regulated by p53. *Oncogene*, **27**, 1562–1571.

43. Banerjee, T., Nath, S. and Roychoudhury, S. (2009) DNA damage induced p53 downregulates Cdc20 by direct binding to its promoter causing chromatin remodeling. *Nucleic Acids Res.*, **37**, 2688–2698.

44. Englert, C., Vidal, M., Maheswaran, S., Ge, Y., Ezzel, R.M., Isselbacher, K.J. and Haber, D.A. (1995) Truncated WT1 mutants alter the subnuclear localization of the wild-type protein. *Proc. Natl. Acad. Sci. USA.*, **92**, 11960–11964.

45. Kim, M.K.-H., McGarry, T.J., O Broin, P., Flatow, J.M., Golden, A.A.-J. and Licht, J.D. (2009) An integrated genome screen identifies the Wnt signalling pathway as a major target of WT1. *Proc. Natl. Acad. Sci. USA*, **106**, 11154–11159.

46. Chang, H., Gao, F., Guillou, F., Taketo, M.M., Huff, V. and Behringer, R.R. (2008) Wt1 negatively regulates beta-catenin signaling during testis development. *Development*, **135**, 1875–1885.

47. Morrison, D.J., Kim, M.K.H., Berkofsky-Fessler, W. and Licht, J.D. (2008) WT1 induction of mitogen-activated protein kinase phosphatase 3 represents a novel mechanism of growth suppression. *Mol. Cancer Res.*, **6**, 1225–1231.

48. Guo, J.K., Menke, A.L., Gubler, M.C., Clarke, A.R., Harrison, D., Hammes, A., Hastie, N.D. and Schedl, A. (2002) WT1 is a key regulator of podocyte function: reduced expression levels cause crescentic glomerulonephritis and mesangial sclerosis. *Hum. Mol. Genet.*, **11**, 651–659.

49. Stanhope-Baker, P., Kessler, P.M., Li, W., Agarwal, M.L. and Williams, B.R. (2004) The Wilms tumor suppressor-1 target gene podocalyxin is transcriptionally repressed by p53. *J. Biol. Chem.*, **279**, 33575–33585.

50. Palmer, R.E., Kotsianti, A., Cadman, B., Boyd, T., Gerald, W. and Haber, D.A. (2001) WT1 regulates the expression of the major glomerular podocyte membrane protein Podocalyxin. *Curr. Biol.*, **11**, 1805–1809.

51. Green, L.M., Wagner, K.J., Campbell, H.A., Addison, K. and Roberts, S.G. (2009) Dynamic interaction between WT1 and BASP1 in transcriptional regulation during differentiation. *Nucleic Acids Res.*, **37**, 431–440.

52. Patek, C.E., Little, M.H., Fleming, S., Miles, C., Charlieu, J.P., Clarke, A.R., Miyagawa, K., Christie, S., Doig, J., Harrison, D.J. *et al.* (1999) A zinc finger truncation of murine WT1 results in the characteristic urogenital abnormalities of Denys-Drash syndrome. *Proc. Natl. Acad. Sci. USA.*, **96**, 2931–2936.

53. Morton, J.P., Timpson, P., Karim, S.A., Ridgway, R.A., Athineos, D., Doyle, B., Jamieson, N.B., Oien, K.A., Lowy, A.M., Brunton, V.A. *et al.* (2010) Mutant p53 drives metastasis and overcomes growth arrest/senescence in pancreatic cancer. *Proc. Natl. Acad. Sci. USA.*, **107**, 246–251.

54. Campeau, E., Ruhl, V.E., Rodier, F., Smith, C.L., Rahmberg, B.L., Fuss, J.O., Campisi, J., Yaswen, P., Cooper, P.K. and Kaufman, P.D. (2009) A versatile viral system for expression and depletion of proteins in mammalian cells. *PLoS One.*, **4**, e6529.

55. Veeman, M.T., Slusarski, D.C., Kaykas, A., Louie, S.H. and Moon, R.T. (2003) Zebrafish prickle, a modulator of noncanonical Wnt/Fz signaling, regulates gastrulation movements. *Curr Biol.*, **13**, 680–685.

56. Veldhoen, N., You, Q., Setzer, D.R. and Romaniuk, P.J. (1994) Contribution of individual base pairs to the interaction of TFIIIA with the Xenopus 5S RNA gene. *Biochemistry*, **33**, 7568–7575.

57. Hartmann, L., Neveling, K., Borkens, S., Schneider, H., Freund, M., Grassman, E., Theiss, S., Wawer, A., Burdach, S., Auerbach, A.D. *et al.* (2010) Correct mRNA processing at a mutant TT splice donor in FANCC

58. Hamilton, T.B., Barilla, B. and Romaniuk, P. (1995) High affinity binding sites for the Wilms' tumour protein WT1 High affinity binding site suppressor protein WT1. *Nucleic Acids Res.*, **23**, 277–284.

59. el-Deiry, W.S., Tokino, T., Velculescu, V.E., Levy, D.B., Parsons, R., Trent, J.M., Lin, D., Mercer, W.E., Kinzler, K.W. and Vogelstein, B. (1993) WAF1, a potential mediator of p53 tumor suppression. *Cell*, **75**, 817–825.

60. Goodfellow, S.J., Rebello, M.R., Toska, E., Zeef, L.A.H., Rudd, S.G., Medler, K.F. and Roberts, S.G.E. (2011) WT1 and its transcriptional cofactor BASP1 redirect the differentiation pathway of an established blood cell line. *Biochem. J.*, **435**, 113–125.

ameliorates the clinical phenotype in patients and is enhanced by delivery of suppressor U1 snRNAs. *Am. J. Hum. Genet.*, **87**, 480–493.